

First determination of anticancer, cytotoxic, and in silico ADME evaluation of secondary metabolites of endemic *Astragalus leucothrix* Freyn & Bornm

Ayşe ŞAHİN YAĞLIOĞLU^{1*}, Duygu GÜNEŞ GÜRBÜZ², Melda DÖLARSLAN³, İbrahim DEMİRTAŞ⁴

¹Department of Chemistry and Chemical Process Technology, Technical Sciences Vocational School, Amasya University, Amasya, Turkey

²Department Chemistry, Faculty Science, University Çankırı Karatekin, Çankırı, Turkey

³Department Biology, Faculty Science, University Çankırı Karatekin, Çankırı, Turkey

⁴Department of Biochemistry, Faculty of Science and Arts, Iğdır University, Iğdır, Turkey

Received: 07.04.2021 • Accepted/Published Online: 05.10.2021 • Final Version: 23.02.2022

Abstract: Isolation and characterization of anticancer activity guided secondary metabolites of endemic *Astragalus leucothrix* Freyn & Bornm were aimed. Aerial parts of the plant were extracted by maceration method in the solvent system methanol-chloroform (1 : 1) at room temperature. The obtained crude extract was dissolved in purified water. Then, the extract was partitioned with *n*-hexane, chloroform, ethyl acetate, and *n*-butanol, respectively. Anticancer activity tests of all the fractions were performed against HeLa and C6 cancer cells. The chloroform fraction that has highest anticancer activity was subjected to chromatographic methods such as column chromatography and thin layer chromatography. Pentyl tetratetracontanoate (1), alfalone (2), 3,6,8-tribromoquinoline (3), and 3,6,8-tribromochromenium (4) molecules were detected from this plant for the first time. The structure determinations of the isolated molecules were elucidated by methods such as 1D and 2D NMR, HPLC - TOF / MS, and GC - MS analysis. Finally, anticancer and cytotoxic activity tests of the compounds were performed. Literature review showed that 3,6,8-tribromochromenium is a new compound. IC₅₀ values of compound 1-2 and compound 3-4 mix were determined to be 4.50 ± 0.10, 2.81 ± 0.00, 4.33 ± 0.00 µM against C6 cell, respectively. The drug likeness properties of 1-4 were obtained by SwissADME. According to Lipinski's rule of five; 2-4 could be a new potential anticancer agent.

Key words: *Astragalus leucothrix*, anticancer activity, cytotoxic activity, in silico ADME, alfalone, C6 cell

1. Introduction

Cancer is a major global public health problem. In addition, the incidence and mortality rates of cancer continue to increase. There will be an estimated 18.1 million new cancer cases and 9.6 million cancer deaths in 2018 [1]. Various systemic treatments such as surgery, chemotherapy, radiotherapy, and hormone therapy are used in cancer treatment [2,3]. Despite these treatment methods, neither a decrease in the number of patients with this disease nor a decrease in the mortality rate is observed [3]. In addition, cancer drugs cause toxicity in normal cells and tissues, causing serious side effects such as vomiting, nausea, hair loss, and resistance development [3-6]. Potential anticancer activities of many medicinal drugs and plant extracts have been investigated in order to avoid these undesirable side effects [3, 7-12]. Therefore, it is extremely important to develop more effective treatments by plants.

Astragalus L. (Fabaceae) taxon is one of the largest genera in the world with 2500–3000 taxa [13-16]. In the studies conducted on *Astragalus* taxa in Turkey, it has been reported that there are 425–450 taxa, 201–224 of which are endemic and the rate of endemism varies between 47% and 50% [16,17].

Astragalus ssp. includes saponins, flavonoids, and polysaccharides as main classes of compounds [18]. Also, the species contents anthraquinones, alkaloids, amino acids, β-sitosterol, and metallic elements [19]. *Astragalus* species are used as hepatoprotective, antioxidative, immunostimulant, antiviral [20], antidiabetic, cardioprotective, antiinflammatory [19], for the treatment of wounds and leukemia [21, 22], and anticancer [23] at folk medicine. Also, immunomodulatory and anticancer activity of *Astragalus* genus were reported in some studies [24-26]. This pharmacological activity has been determined to be caused by three groups of chemical substances: polyholosites, saponins, and phenolics [20]. To our knowledge, there is no study about the anticancer activity and isolation of endemic *A. leucothrix* Freyn & Bornm. Thus, the main purpose of the research was to investigate the isolation, structural elucidation, biological activities, and in silico ADME evaluation.

* Correspondence: aysesahin1@gmail.com

2. Materials and methods

2.1. Chemicals

Fetal bovine serum, penicillin/streptomycin, and Dulbecco's modified Eagle's medium-high glucose were purchased from Sigma-Aldrich GmbH. (Germany). Methanol (MeOH), *n*-hexane, chloroform (CHCl₃), ethyl acetate (EtOAc), and *n*-butanol (BuOH) used in HPLC analysis and extraction were HPLC grade and purchased from Merck. LDH Cell Cytotoxicity Assay (Roche 04 744 926 001, Germany) and BrdU ELISA Assay (Cat. No. 11 647 229 001, Germany) were supplied from Roche.

2.2. Plant material

A. leucothrix Freyn & Bornm was collected from Yapraklı District (Çankırı, Turkey) in June 2016. The identification of the plant samples was confirmed by botanist Melda DÖLARSLAN. The plants were stored in the Herbarium of Biology Department, Ankara University, Turkey (Herbarium number: ANK 60526).

2.3. Extraction and isolation

The dry plant (1 kg) was subjected to maceration method in MeOH-CHCl₃ (12 L; 1 : 1) to 2 days extraction at room temperature and the procedure was repeated three times. The resulting mixture was then filtered and the solvent was removed in a rotary evaporator. The crude extract was dissolved in purified water (1 L) and was partitioned with *n*-hexane, CHCl₃, EtOAc, and *n*-BuOH fraction, respectively, and then the solvents were removed to give *n*-hexane (9.42 g), CHCl₃ (3.73 g), EtOAc (2.40 g), *n*-Butanol (11.79 g), and water (14.85 g) fractions within in the yield of 5.87%, 0.94%, 0.37%, 0.24%, 1.17%, and 1.48%, respectively. CHCl₃ fraction (3.50 g) was chromatographed by using silica gel column chromatography to give 556 fractions (20 mL, each). The *n*-hexane 1-28 with *n*-hexane-CHCl₃ (10%), fraction 29-77 with *n*-hexane-CHCl₃ (20%); fraction 78-235 with CHCl₃; fraction 236-299 with acetone-CHCl₃ (5%); fraction 300-334 with acetone-CHCl₃ (10%); fraction 335-365 with acetone-CHCl₃ (15%); fraction 366-399 with acetone- CHCl₃ (50%); fraction 400-423 with acetone-CHCl₃ (70%); fraction 424-457 with acetone; fractions 458-556 with methanol (MeOH) were eluted. Tubes 114 to 174 were combined by thin layer chromatography. The fractions were subjected to column chromatography with *n*-hexane-CHCl₃ (50%) again. In the column chromatography was collected 116 fractions. Compound **1** (18 mg), compound **2** (82 mg), and compound **3-4** mix (15.6 mg) were isolated from this column.

2.4. Determination of anticancer assays

The extract, fractions, and pure compounds were investigated for their anticancer activities against human cervical adenocarcinoma (HeLa) and rat glioma cells (C6) by using BrdU ELISA assays. The tested samples and 5-FU were dissolved in dimethyl sulfoxide (DMSO). Then the stock solution was diluted with Dulbecco's Modified Eagle Medium (DMEM). DMSO concentration is below 0.1% in stock solutions. The anticancer activity tests and cell culture study were performed according to the literature [27,28]. The results are means ± SD of six values.

2.5. Determination of cytotoxic assay

The cytotoxic activities of the test substances were determined according to the manufacturer's procedure using LDH cell cytotoxicity assay and cytotoxicity % was calculated [29].

2.6. Physicochemical and pharmacokinetic properties for computational methods

The SwissADME website was written in HTML, PHP5, and JavaScript, whereas the backend of computation was mainly coded in Python 2.7. The use of additional libraries or software for specific tasks is mentioned in the corresponding paragraph.

The molecule inputted through the sketcher Marvin JS (version 16.4.18, 2016, www.chemaxon.com) are converted into SMILES by JChem Web Services (version 14.9.29, 2013, www.chemaxon.com) installed on one of our servers. This on-the-fly conversion allows seamless paste of SMILES in the input list. The user has the possibility to edit this list as a standard text, e.g., to modify SMILES or add a name to the molecule.¹ Upon calculation submission by clicking the "Run" button, the SMILES of each molecule is canonicalised by OpenBabel (version 2.3.0, 2012, http://openbabel.org) and processed individually [30]. Drug-likenesses and molecular property predictions of compounds are determined by the programme at http://www.molsoft.com/mprop/mprop.cgi.

2.7. Statistical analysis and determination of IC₅₀ values

Statistical analyses were used to evaluate anticancer and cytotoxic activity results by one-way ANOVA test. The results are means ± SD of six values. Differences between groups were determined by ANOVA method ($p < 0.01$). The IC₅₀ values were determined using ED50 plus v1.0.

¹ www.nature.com/scientificreports/SCientific REpOrtS | 7:42717 | DOI: 10.1038/srep42717

3. Results and discussion

3.1. Isolation and characterization

Isolation procedure was started with CHCl_3 fraction which showed the highest anticancer activity. Three compounds were isolated and identified by spectroscopic methods from the CHCl_3 fraction. After the TLC analysis, combined fractions 66-81 (274.6 mg) gave the compound **1** (pentyl tetracontanoate), which was determined by using 1D and 2D Nuclear Magnetic Resonance (NMR) spectroscopy (Figures S1–S3). When the proton (^1H) NMR spectrum (600 MHz, CDCl_3) was examined, two triplet peaks at 0.89 were observed to belong to the terminal methyl proton. The proton of H-1' was at δ 4.06 and the H-2 proton was resonated as a triplet at δ 2.28. The proton of H-2' was signalled at δ 1.62 and the proton of H-3 at δ 1.61. Forty-six CH_2 groups were determined by utilizing the ^1H NMR spectrum integration values (Figure 1).

When the heteronuclear multiple-bond correlation (HMBC) NMR spectrum of compound **1** was examined, it was determined that the H-8 proton (shown pink) interacts with C-9 and C-7 (carbonyl carbon) carbons. The H-5 proton (shown in red) was shown to correlate with the C-3, C-4, and C-7 carbons (Figure S1). When the carbon (^{13}C) NMR spectrum and distortionless enhancement by polarization transfer (DEPT; 150 MHz, CDCl_3) was examined, the presence of the carbonyl group was determined in δ 173.94 (Figure S2). C-5 carbon was found to be resonance in δ 64.16. The methyl carbons were observed at δ 14.00 (Figures S2 and S3). The compound **1** was isolated from *A. leucothrix* and *Astragalus* ssp. for the first time.

After the TLC analysis, fractions 114-174 (82 mg) gave compound **2** (6-hydroxy-7,4'-dimethoxy isoflavone; alfalone; Figure 2) which was determined by the 1D and 2D NMR and HPLC / TOF - MS analysis (Figures S4–S12) [31–33]. Compound **2** was identified as isoflavone (alfalone) that isolated for the first time as a natural product [31]. Alfalone is found in many plants such as *Medicago truncatula* [34], *Trifolium pratense* and *Machaerium isadelphum* [35], and *Machaerium isadelphum* [36]. However, **2** was isolated for the first time from *A. leucothrix* and *Astragalus* ssp. In addition, a large number of isoflavone-type compounds have been isolated from *Astragalus* species. For example, acicerone [37] from *Astragalus cicer*, maackiain from *Astragalus trojanus* [38], diadzen, genisten, and 7-hydroxy-3',5'-dimethoxyisoflavone from *Astragalus peregrines* [39], 5,5'-dihydroxy-3'-methoxy-isoflavone-7-O- β -D-glucoside, genistin, sissotrin, and 5,4'-dimethoxy-isoflavone-7-O- β -D-glucopyranoside from *Astragalus lycius* Boiss [40].

HPLC/TOF-MS analysis of compound **2** gave $[\text{M}]^+$ peak at 297.0981 ($\text{C}_{17}\text{H}_{14}\text{O}_5$) (Figures S4 and S5). The singlet peak observed at δ 7.91 in the ^1H NMR spectrum of compound **2** is characteristic for the H-2 proton in the isoflavone skeleton [39]. The singlet peak in the ^1H NMR spectrum (Table S1) that were observed in δ 3.83 and 4.01 indicates the methoxy protons linked to the C-4' and C-7 carbons, respectively, in HMBC spectrum. Protons in the A2X2 system (δ 6.97, dd, 2H, $J = 2.0, 8.0$ Hz; δ 7.50, dd, 2H, $J = 2.0, 8.0$ Hz) are observed to interact with the C-4' carbon-linked methoxy protons. In the ^1H NMR spectrum peak at δ 6.27 (1H, s) belongs to the -OH peak due to the D_2O exchange (Figure S8). Peaks at δ 7.65 and

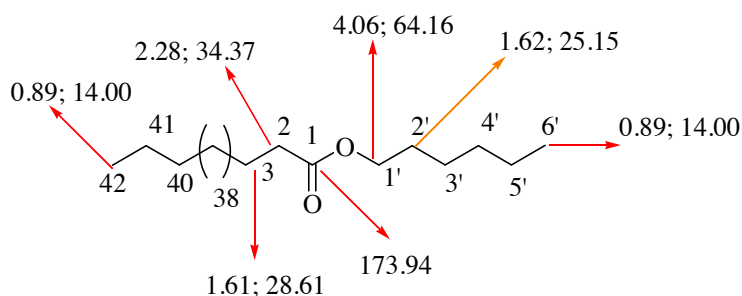


Figure 1. The chemical structure of compound **1** (1st value is proton, 2nd value is carbon values.)

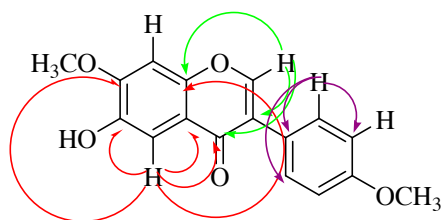


Figure 2. Key HMBC correlation of compound **2**.

6.97 (1H) assigned to the H-5 and H-8 protons, respectively (Figure S6). When the ^{13}C NMR spectrum of **2** is examined, a signal for the carbonyl group is observed at δ 175.65 and two methoxy peaks at δ 55.46 and 56.66 are observed (Figure S9). When the DEPT of **2** is examined, two CH and five CH signals are observed (Figure S10).

When the HMBC NMR spectrum of compound **2** was examined, it was determined that the H-2 proton (shown green) interacts with C-3, C-4 (carbonyl carbon), and C-9 carbons. The H-5 proton (shown in red) was shown to correlate with the C-4, C-6, C-7, C-9, and C-10 carbons. The H-2' proton (shown in purple) appears to interact with the C-1', C-3', and C-6' carbons (Figure S7). HSQC spectrum of **2** gave the correlation of peaks; at δ 7.92 with the carbon at δ 152.04; δ 7.50 with the carbon at δ 130.58; at δ 7.65 with the carbon at δ 104.96; at δ 6.97 with the carbon at δ 102.74; at δ 6.97 with the carbon at δ 114.38; at δ 4.01 with the carbon at δ 56.66; and at δ 3.83 with the carbon in δ 55.46 (Figure S11). The COSY spectrum of **2** resulted the correlation, H-2', 6' at δ 7.50 (2H, $J = 2.0, 8.0$ Hz) with H-3', 5' at δ 6.97 (2H, $J = 2.0, 8.0$ Hz) (Figure S12). Thus, the spectral evidence resulted that compound **2** was identified as alalone which is a known compound [33-35], but it was isolated and characterized first time from this plant.

The fractions 114-174 (15.6 mg) were seen as a pure compound in TLC, HPLC/TOF-MS and GC-MS analyses (Figures S13 and S14). However, 3,6,8-tribromoquinoline (**3**) and 3,6,8-tribromochromenium (**4**) mix were obtained which were determined by 1D and 2D NMR analysis (Figures S15–S21, Table 1). When the spectra at Figure S16 and S17 are examined;

Table 1. NMR data of compounds **3-4** (CDCl_3 , 600 and 150 MHz); IC_{50} values and cytotoxicity (%) of the compounds.

Compound 3 (3,6,8-tribromoquinoline)					
	Detected	Literature (ppm) [41-43]	Detected (ppm)	Literature (ppm) [41-43]	Detected/literature
2	9.00 (1H, <i>bs</i>)	8.99 (1H, <i>d</i> *)	152.47	153.42	CH/ CH
3	-	-	119.24	120.06	C
4	8.24 (1H, <i>bs</i>)	8.20 (1H, <i>d</i> *)	136.64	137.51	CH/ CH
5	-	-	121.22	121.97	C
6	7.88 (1H, <i>bs</i>)	7.86 (1H, <i>d</i> *)	128.76	129.57	CH/ CH
7	-	-	126.03	126.77	C
8	8.15 (1H, <i>bs</i>)	8.14 (1H, <i>d</i> ')	136.31	137.15	CH/ CH
9	-	-	142.36	143.18	C
10	-	-	130.72	131.50	C
Compound 4 (3,6,8-tribromobenzopyrylium)					
	Detected (ppm)	Literature [41-43]	Detected (ppm)	Literature (ppm) [41-43]	Detected/literature
2	9.00 (1H, <i>bs</i>)	8.99 (1H, <i>d</i> *)	174.21	169.20–179.60 ⁴¹	CH/ CH
3	-	-	119.31	120.06	C
4	8.24 (1H, <i>bs</i>)	8.20 (1H, <i>d</i> *)	136.64	137.51	CH/ CH
5	-	-	121.27	121.97	C
6	7.88 (1H, <i>bs</i>)	7.86 (1H, <i>d</i> *)	128.76	129.57	CH/ CH
7	-	-	126.03	126.77	C
8	8.15 (1H, <i>bs</i>)	8.14 (1H, <i>d</i> *)	136.31	137.15	CH/ CH
9	-	-	152.47	155.90–167.00 ⁴¹	C
10	-	-	130.72	131.50	C
		HeLa cell	C6 cell	Cytotoxicity (%)	
Compound 1		72.35 \pm 0.51 ^a	4.50 \pm 0.10 ^a	24.25 \pm 0.01 ^c	
Compound 2		22.07 \pm 0.21 ^b	2.81 \pm 0.00 ^b	43.02 \pm 0.02 ^a	
Compound 3+4		73.22 \pm 0.25 ^a	4.33 \pm 0.00 ^a	4.05 \pm 0.01 ^d	
5-FU		16.32 \pm 0.11 ^c	5.8 \pm 0.10 ^c	39.02 \pm 0.03 ^b	

^aSignals specified as doublets appear as broad singlets in the article [42].

two peaks were observed to overlap at 152.47, 136.64, 130.72, 128.76, 121.22, and 119.31 ppm. In addition, when Figure S17 was examined; another peak was detected at 174.21 ppm. When Kar et al., 2021 was examined, it was determined that the C2 carbon in benzopyrylium ions had a resonance between 169.20 and 179.60 ppm. Also, carbon C9 resonates between 155.90 and 167.00 ppm depending on the substituent at C6 and/or C8 [41]. However, all peaks except carbons C2 and C9 are compatible with compound 3 (3,6,8-tribromoquinoline)[42-43]. Considering the peaks, the structure was determined to be compound 4 (3,6,8-tribromobenzopyrylium, Table 1). In addition, when the spectrums at Figure S16 are examined; nine peaks were determined 152.47, 142.36, 136.64, 136.31, 130.72, 128.76, 126.03, 121.22, and 119.31 ppm. The peaks are compatible with compound 3 [42-43].

The quinoline skeleton is found in a variety of natural compounds and synthetic derivatives. It has many biological activities such as antimalarial, antibacterial, antifungal, anthelmintic, cardiotoxic, anticonvulsant, anti-inflammatory, and analgesic activity [44]. However, quinolone derivatives were isolated from many plants such as *Ephedra pachyclada* ssp. *sinaica* [45], *Haplophyllum foliosum*, *Haplophyllum pedicellatum* [46], *Solidago canadensis* [47], *Eremophila microtheca* [48], *Lunasia amara* [49], and *Pitaviaster haplophyllus* [50].

In addition, the first naturally occurring bromo-quinoline alkaloid was isolated from the marine bryozoan *Flustra foliacea* (L.) [51].

In ^1H NMR spectrum (600 MHz, CDCl_3 , Figure S15, Table 1) of compound 3-4 mix, H-2 proton peak at δ 9.00 (2H, s), H-4 proton at δ 8.24 (2H, s), H-6 proton at δ 7.88 (2H, s), and H-8 proton at δ 8.15 (2H, s) were determined [42]. In ^{13}C NMR spectrum and HPLC-TOF/MS analysis of compound 3-4 mix, compound 3 was observed as $[\text{C}_9\text{H}_4\text{Br}_3\text{N}]^+$ and $[\text{M}]^+$ peak m/z at 367.8055 (Figure S20). At the same time, compound 4 was detected as $[\text{C}_9\text{H}_4\text{Br}_3\text{O}]^+$, $[\text{M}]^+$ peak m/z at 365.8074 (Figure S20). The nitrogen rule in mass spectrometry states that (organic) molecules containing no or an even number of nitrogen atoms will have even masses, and molecules containing an odd number of nitrogen atoms will have odd masses [52]. Thus, the fact that the molecular ion peak in the mass spectrum is a single number supports the presence of nitrogen atom in the structure. In addition, when the mass spectrum was examined, three bromine atoms were observed in both molecules (Figure S20)[53]. ^{13}C and DEPT NMR spectra of compound 3 (150 MHz, CDCl_3) gave nine signals at δ 152.47, 119.24, 136.64, 121.22, 128.76, 126.03, 136.31, 142.36, and 130.72, which were assigned to carbons C-2, C-3, C-4, C-5, C-6, C-7, C-8, C-9, and C-10, respectively [42]. In the HMBC spectrum (600 MHz, CDCl_3) in Figure 3, the H-2 proton (shown in red) was found to interact with the C-3, C-4, and C-9 carbons. The H-4 proton (shown in green) correlates with the C-2, C-3, C-5, and C-10 carbons. The H-8 proton (shown in pink) interacts with C-6, C-7, C-9, and C-10 carbons (Figures 3 and S21). When the HSQC spectrum (600 MHz, CDCl_3) in Figure S19 was examined, the proton in δ 9.00 ppm with carbon at δ 152.47 ppm, the proton in δ 8.24 ppm with carbon in δ 136.64 ppm, the proton in δ 8.15 ppm with the carbon in δ 136.31 ppm, and the proton in δ 7.88 ppm with the carbon in the carbon δ 128.66 ppm were seen to be correlated. The interactions overlap with compound 3. Bromine ranks 44th among the elements found in the earth's crust. There are many organobromine compounds synthesized by living organisms or formed as a result of natural abiotic processes [54]. Because of their similar physical and chemical properties, bromides are commonly found in the environment together with sodium chloride in smaller amounts. Br has been shown to be a new and important trace element for humans and animals [55]. Although various plant species can accumulate high concentrations of Br, to our knowledge, their role in plants has not been established [56]. In marine plants (for example, *Bonnemaisonia hamifera*, *Laurencia* species), marine animals (for example, sponges, bryozoans, corals), mammals (for example, cat and rat), abiogenic sources, plants (for example, rapeseed,

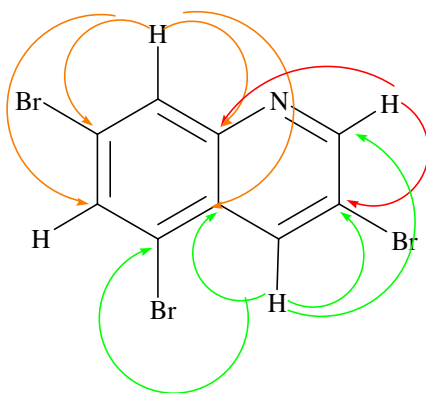


Figure 3. Key HMBC correlation of compound 3-4 mix.

mustard, cabbage, Chinese cabbage, broccoli, pak-choi, alyssum, wild mustard, turnip, radish), fungi and lichen, bacteria (for example, *Bacillus subtilis*, *Chromobacterium* species), and insects are naturally found organobromine compounds [57]. However, the compound 3 and 4 were isolated from *A. leucothrix* and *Astragalus* ssp. for the first time.

3.2. Anticancer activity

The anticancer activities of MeOH: CHCl₃ extract, *n*-hexane, CHCl₃, EtOAc, *n*-Butanol and water fractions and 5-FU that were used as a standard against C6 and HeLa cell were investigated (Figure 4). As a result of the tests performed, an increase in the activity of all extracts due to dose increase was observed. Activity at 100 µg/mL concentration against HeLa cell (Figure 4): CHCl₃ fraction > 5-FU > *n*-hexane fraction > EtOAc fraction > MeOH: CHCl₃ extract > *n*-BuOH fraction > water fraction. When cancer activity results were examined in both cells, the most active fraction was found to be chloroform fraction. The highest activity against C6 cells was observed in *n*-hexane and chloroform fractions (Figure 4). Activity at 100 µg/mL concentration against C6 cell: *n*-hexane fraction > CHCl₃ fraction > MeOH: CHCl₃ extract > 5-FU > EtOAc fraction > water fraction > *n*-BuOH fraction.

In cytotoxicity studies on *Astragalus chrysochlorus* extracts, the highest effect was observed in chloroform extract. This extract was followed by ethyl acetate, ethanol, *n*-hexane, and aqueous ethanol extracts [58]. Similarly, in our study, the highest effect was observed in chloroform extract. This extract was followed by *n*-hexane extract. We performed GC-MS analyses of *n*-hexane and chloroform extracts of *A. leucothrix* (Table 2). In the *n*-hexane extract, palmitic acid, linolenic acid, and linoleic acid were main components. Palmitic acid, linolenic acid, and behenic acid were major compounds in

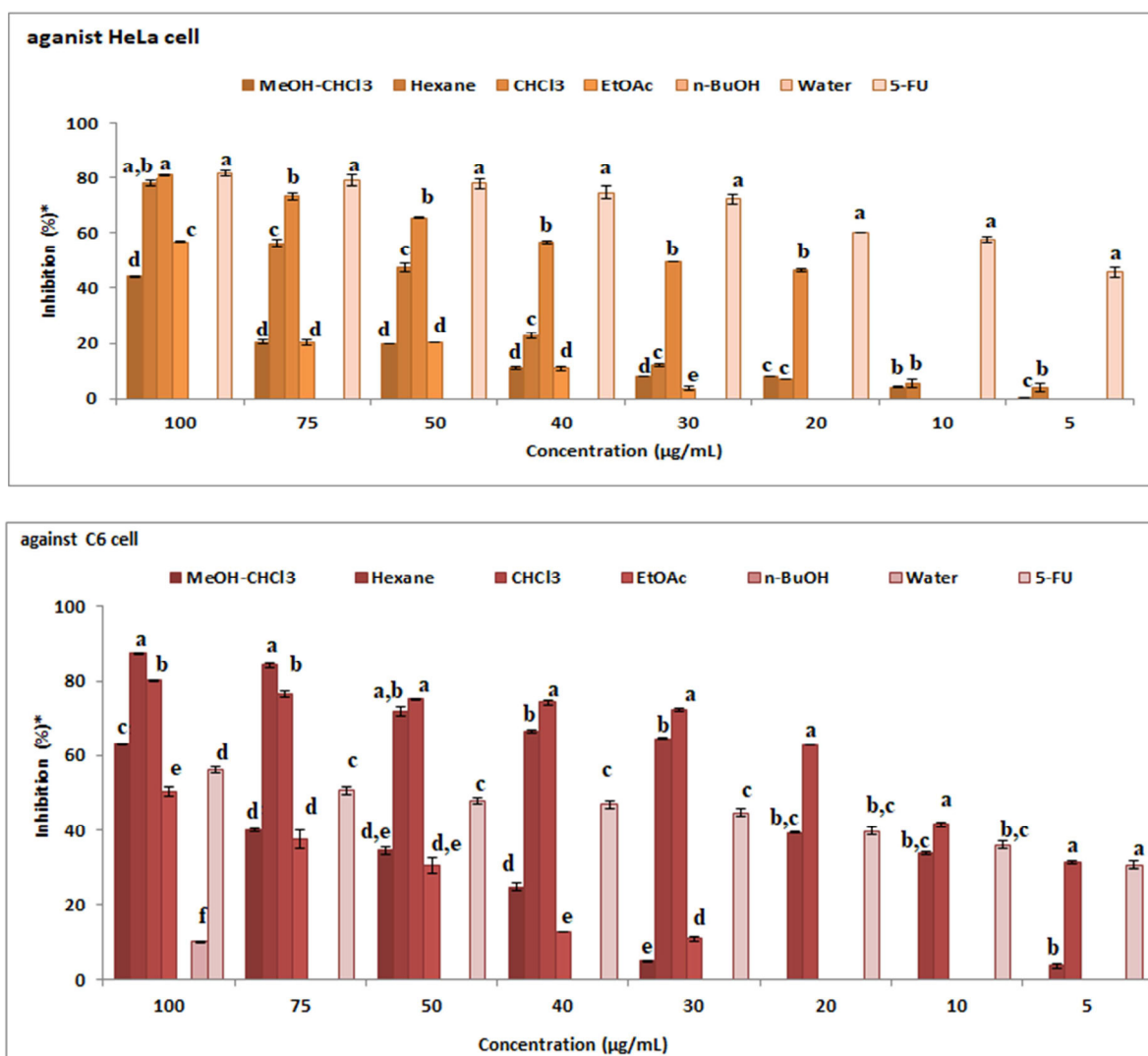


Figure 4. The anticancer activity of extracts against C6 and HeLa cell (* tests repeated three times and twice).

Table 2. GC-MS analysis results of the *n*-hexane and chloroform extracts of *A. leucothrix*.

No	RT	Isomer	Compound name	Area%	
				<i>n</i> -Hexane	CHCl ₃
Saturated Fatty Acids (SFAs)					
1	19.834	C ₁₂ :0	Lauric acid	-	0.86
2	22.912	C ₁₄ :0	Myristic acid	1.36	1.04
3	27.650	C ₁₆ :0	Palmitic acid	19.72	18.30
4	32.583	C ₁₈ :0	Stearic acid	4.41	5.02
5	34.854	C ₂₀ :0	Arachidic acid	3.14	3.27
6	37.320	C ₂₂ :0	Behenic acid	2.56	11.27
7	45.577	C ₂₃ :0	Tricosylic acid	-	2.50
8	40.622	C ₂₄ :0	Lignoceric acid	-	4.89
Subtotal				31,19	57,15
Polyunsaturated Fatty Acids (PUFAs)					
9	32.193	C ₁₈ :2	Linoleic acid	11.41	4.81
10	32.302	C ₁₈ :3	Linolenic acid	28.32	13.30
Subtotal				39.73	18.11
Other Components					
11	32.445		3,7,11,15-Tetramethyl-2-hexadecen-1-ol	2.42	1.53
12	36.834		Behenic alcohol	-	1.76
13	39.998		Heptacosane	2.39	2.78
14	44.616		Nonacosane	10.31	8.79
15	51.992		Hentriacontane	2.90	9.85
16	64.214		γ-Sitosterol	11.06	-
17	53.336		Octacosanoic acid, methyl ester	-	0.36
Subtotal				26.18	25.07
General Total				97.1	100.3

chloroform extracts. PUFA fatty acids are used in chemotherapy. They also increase the effectiveness of chemotherapeutic drugs and may reduce chemotherapy or cancer side effects. Linolenic acid in the chloroform extract inhibited various cancer cells such as GOTO, SK-N-DZ, DU145, A-549, PC-3, 36B10 cells [59]. Also, palmitic acid has anticancer activity against human leukemic cell line (MOLT-4), colon 26 murine tumour cells, and human breast cancer (MCF-7). It is also known that the crude extracts are more effective than their pure compounds for pharmacologically. This effect is thought to be due to the synergistic effect of many molecules in the extracts [60].

The anticancer activities of the isolated compound 1-2, compound 3-4 mix, and 5-FU used as standard were examined against the HeLa as a result of the tests (Figure 5), an increase was observed in all molecules (except compound 3-4 mix) due to dose increase. Among the isolated molecules, the highest activity against the HeLa cell was observed in the compound 2.

Activity at a concentration of 100 µM is as follows: 5-FU > compound 2 > compound 1 > compound 3-4 mix. As a result of anticancer activity tests of compound 1-2, compound 3-4 mix, and 5-FU against C6 cells (Figure 5), an increase was observed in all molecules due to dose increase. The highest activity against the C6 cell between the isolated molecules and the 5-FU was observed in the compound 2. Cell selective activity against C6 cells was observed in all isolated molecules. The activity at 100 µM concentration is compound 2 > 5-FU > compound 3-4 mix > compound 1. The anticancer activities of the isolated compound 1-2, compound 3-4 mix, and 5-FU used as standard were examined against the HeLa and C6 cells. The IC₅₀ values of these compounds are given in Table 2.

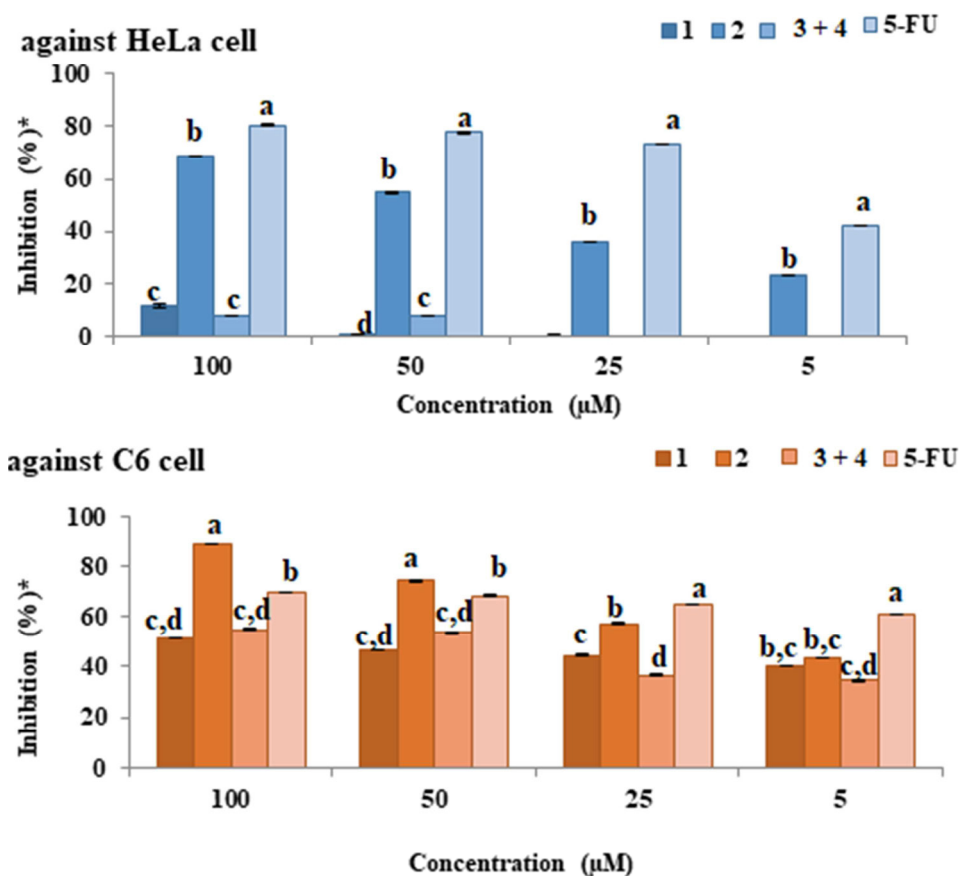


Figure 5. The anticancer activity of the compounds against C6 and HeLa cell (* tests repeated three times and twice).

As in this study, the isolated compounds and extracts from *Astragalus* species such as *Astragalus tribuloides* [60], *Astragalus hamosus* [60-62], *Astragalus membranaceus* [25, 63-64], *Astragalus ovinus* [65], *Astragalus vogelii* [66], *Astragalus complanatus* [67] have anticancer activity.

3.3. Cytotoxic activity

C6 cells were used to determine cytotoxic activity. 100 µg/mL concentration, which is the highest dose used in the anticancer activity tests, was also studied during the experiment. 5-FU was used as a positive control. Test results were given in Table 1. The cytotoxicity values of the samples are relatively small (except compound 2) compared to 5-FU. Especially compound 3-4 mix is less toxic than 5-FU.

3.4. Drug likeness properties

The number of hydrogen bond acceptors (n-ON) and donors (n-OH/NH) are within the Lipinski's rules, n-ON < 10 and n-OH/NH < 5. The calculated log P must be smaller than 5. In our study, the log P values of compound 2-4 were smaller than 5. The molecular weight of the compounds is in the range of 298.29 g/mol and 719.30 g/mol, respectively. The blood-brain barrier (BBB) score: 6-High, 0-Low [68]. The BBB score of compound 1-4 ranges from 3.23 to 4.28. Compound 1-4 can cross the BBB. Synthetic accessibility score of the compounds are from 1 (very easy) to 10 (very difficult). Synthetic accessibility of all the compounds is in the range of 1.79 and 6.77. Topological polar surface area (TPSA) must be <70 Å². TPSA values of all the compounds were smaller than 70 Å² (Tables 3 and 4).

The solubility (log S) scale value ranges between -10 (insoluble), -6 (poorly soluble), -4 (soluble), -2 (very soluble), and 0 (highly soluble). The solubility values of compound 1-4 were -16.56, -3.77, -5.36, and 5.10, which respectively correspond to insoluble, soluble, moderately soluble, and moderately soluble. The more negative the skin permeation (log Kp) the less the skin-permeant the molecule. For example, Diclofenac is a good topic antiinflammatory with a predicted log Kp of -4.96 (cm/s), while Ouabain has little chance to cross skin with a predicted log Kp of -10.94 (cm/s). The log Kp values of compound 1-4 were 6.62, -6.15, -5.51, and -5.83 cm/s, respectively. The Kp values showed that compound 2-4

Table 3. Physicochemical properties, lipophilicity, solubility, pharmacokinetics, drug likeness, and medicinal chemistry of compound 1-4 predicted using Swiss ADME.

No	Physicochemical properties	Lipophilicity	Water solubility	Pharmacokinetics	Drug likeness	Medicinal chemistry
1	Formula: C ₄₉ H ₉₈ O ₂ Molecular weight: 719.30 g/mol Num. heavy atoms: 51 Num. arom.heavy atoms: 0 Fraction Csp ³ :0.98 Num. rotatable bonds: 47 Num. H-bond acceptors: 2 Num. H-bond donors: 0 Molar Refractivity: 238.94 TPSA: 26.30 Å ²	Log P _{o/w} (iLOGP): 11.92 Log P _{o/w} (XLOGP3): 24.38 Log P _{o/w} (WLOGP): 18.12 Log P _{o/w} (MLOGP): 10.48 Log P _{o/w} (SILICOS-IT): 19.98 Consensus Log P _{o/w} : 16.98	Log S (ESOL): -16.56 Solubility: 1.99e-14 mg/ml ; 2.77e-17 mol/l Class: Insoluble Log S (Ali): -25.40 Solubility: 2.85e-23 mg/ml ; 3.96e-26 mol/l Class: Insoluble Log S(SILICOS-IT): -18.49 Solubility: 2.33e-16 mg/ml ; 3.24e-19 mol/l Class: Insoluble	GI absorption:Low P-gp substrate: Yes CYP1A2 inhibitor: No CYP2C19 inhibitor:No CYP2C9 inhibitor:No CYP2D6 inhibitor:No CYP3A4 inhibitor:No Log Kp (skin permeation): 6.62 cm/s	Lipinski: No; 2 violations: MW>500, MLOGP>4.15 Ghose: No; 4 violations: MW>480, WLOGP>5.6, MR>130, #atoms>70 Veber: No; 1 violation: Rotors>10 Egan: No; 1 violation: WLOGP>5.88 Muegge: No; 3 violations: MW>600, XLOGP3>5, Rotors>15 Bioavailability Score: 0.17	PAINS: = 0 alert Brenk: 0 alert Leadlikeness: No; 3 violations: MW>350, Rotors>7, XLOGP3>3.5 Synthetic accessibility: 6.77
2	Formula: C ₁₇ H ₁₄ O ₅ Molecular weight: 298.29 g/mol Num. heavy atoms: 22 Num. arom.heavy atoms: 16 Fraction Csp ³ :0.12 Num. rotatable bonds: 3 Num. H-bond acceptors: 5 Num. H-bond donors: 1 Molar Refractivity: 82.93 TPSA: 68.90 Å ²	Log Po/W (iLOGP): 2.95 Log Po/W (XLOGP3): 2.77 Log Po/W (WLOGP): 3.18 Log Po/W (MLOGP): 1.01 Log Po/W (SILICOS-IT): 3.55 Consensus Log Po/W: 2.69	Log S (ESOL): -3.77 Solubility: 5.01e-02 mg/ml ; 1.68e-04 mol/l Class: Soluble Log S (Ali): -3.87 Solubility: 4.00e-02 mg/ml ; 1.34e-04 mol/l Class: Soluble Log S(SILICOS-IT): -5.80 Solubility: 4.74e-04 mg/ml ; 1.59e-06 mol/l Class: Moderately soluble	GI absorption: High P-gp substrate:No CYP1A2 inhibitor: Yes CYP2C19 inhibitor: No CYP2C9 inhibitor: Yes CYP2D6 inhibitor: Yes CYP3A4 inhibitor: Yes Log Kp (skin permeation): -6.15 cm/s	Lipinski: Yes; 0 violation Ghose: Yes Veber: Yes Egan: Yes Muegge: Yes Bioavailability Score: 0.55	PAINS: 0 alert Brenk: 0 alert Leadlikeness: Yes Synthetic accessibility: 3.04
3	Formula: C ₉ H ₄ Br ₃ N Molecular weight: 365.85 g/mol Num. heavy atoms: 13 Num. arom.heavy atoms: 10 Fraction Csp ³ :0.00 Num. rotatable bonds: 0 Num. H-bond acceptors: 1 Num. H-bond donors: 0 Molar Refractivity: 64.84 TPSA: 12.89 Å ²	Log P _{o/w} (iLOGP): 2.79 Log P _{o/w} (XLOGP3): 4.26 Log P _{o/w} (WLOGP): 4.52 Log P _{o/w} (MLOGP): 3.93 Log P _{o/w} (SILICOS-IT): 4.44 Consensus Log P _{o/w} : 3.99	Log S (ESOL): -5.36 Solubility: 1.59e-03 mg/ml; 4.35e-06 mol/l Class: Moderately soluble Log S (Ali): -4.24 Solubility: 2.09e-02 mg/ml; 5.72e-05 mol/l Class: Moderately soluble Log S(SILICOS-IT): -6.21 Solubility: 2.28e-04 mg/ml ; 6.22e-07 mol/l Class: Poorly soluble	GI absorption: High P-gp substrate: No CYP1A2 inhibitor:Yes CYP2C19 inhibitor: Yes CYP2C9 inhibitor:No CYP2D6 inhibitor:No CYP3A4 inhibitor:No Log Kp (skin permeation): -5.51 cm/s	Lipinski: Yes; 0 violation Ghose: No; 1 violation: #atoms<20 Veber: Yes Egan: Yes Muegge: No; 1 violation: Heteroatoms <2 Bioavailability Score: 0.55	PAINS: 0 alert Brenk: 0 alert Leadlikeness: No; 2 violations: MW>350, XLOGP3>3.5 Synthetic accessibility: 1.79

Table 3. (Continued).

4	<p>Formula: C₉H₄Br₃O Molecular weight: 367.84 g/mol Num. heavy atoms: 13 Num. arom.heavy atoms: 10 Fraction Csp³: 0.00 Num. rotatable bonds: 0 Num. H-bond acceptors: 1 Num. H-bond donors: 0 Molar Refractivity: 63.72 TPSA: 13.14 Å²</p>	<p>Log P_{o/w} (iLOGP): -2.05 Log P_{o/w} (XLOGP3): 3.82 Log P_{o/w} (WLOGP): 5.00 Log P_{o/w} (MLOGP): 3.93 Log P_{o/w} (SILICOS-IT): 3.16 Consensus Log P_{o/w}: 2.77</p>	<p>Log S (ESOL): -5.10 Solubility: 2.95e-03 mg/ml ; 8.01e-06 mol/l Class: Moderately soluble Log S (Ali): -3.79 Solubility: 5.95e-02 mg/ml ; 1.62e-04 mol/l Class: Soluble Log S(SILICOS-IT): -5.30 Solubility: 1.83e-03 mg/ml ; 4.98e-06 mol/l Class: Moderately soluble</p>	<p>GI absorption: High P-gp substrate: Yes CYP1A2 inhibitor: No CYP2C19 inhibitor: No CYP2C9 inhibitor: No CYP2D6 inhibitor: No CYP3A4 inhibitor: No Log Kp (skin permeation): -5.83 cm/s</p>	<p>Lipinski: Yes; 0 violation Ghose: No; 1 violation: #atoms < 20 Veber: Yes Egan: Yes Muegge: No; 1 violation: Heteroatoms < 2 Bioavailability Score: 0.55</p>	<p>PAINS: 0 alert Brenk: 1 alert: charged_oxygen_sulfur Leadlikeness: No; 2 violations: MW > 350, XLOGP3 > 3.5 Synthetic accessibility: 2.81</p>
---	--	--	--	--	--	---

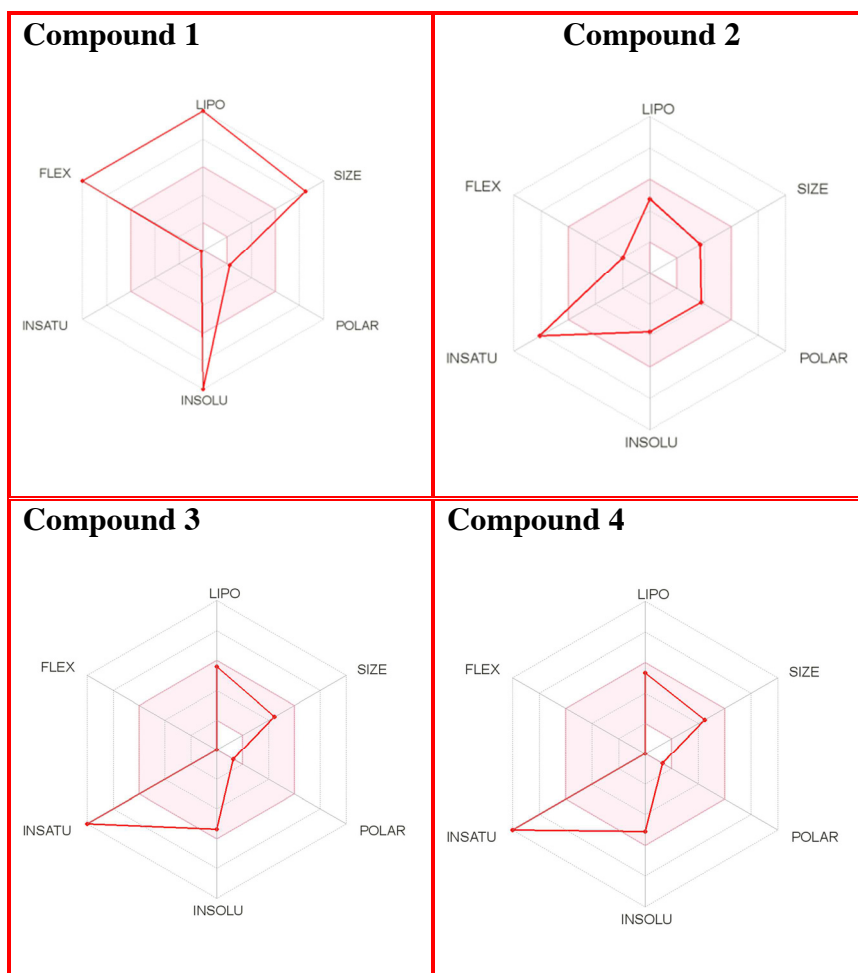


Figure 6. The bioavailability radar of the compounds 1-4.

and 130 \AA^2 , solubility: $\log S$ not higher than 6, saturation: fraction of carbons in the sp^3 hybridization not less than 0.25, and flexibility: no more than 9 rotatable bonds. In this example, compound 2-4 are predicted orally bioavailable, because of being flexible, polar, and small size. Bioavailability radar of compound 1-4 is demonstrated in Figure 6.

Acknowledgement

This study was funded by the Scientific and Technological Research Council of Turkey (TÜBİTAK) [grant number 114Z152].

References

1. Bray F, Ferlay J, Soerjomataram I, Siegel RL, Torre LA et al. Global cancer statistics 2018: GLOBOCAN Estimates of Incidence and Mortality Worldwide for 36 Cancers in 185 Countries. *CA: A Cancer Journal for Clinicians* 2018; 68: 394–424. doi: 10.3322/caac.21492
2. Damyanov C, Maslev I, Pavlov V, Avramov L. Conventional treatment of cancer realities and problems. *Annals of Complementary and Alternative Medicine* 2018; 1: 1002-1011.
3. Singh SP, Mishra A, Shyanti RK, Singh RP, Acharya A. Silver nanoparticles synthesized using *Carica papaya* leaf extract (AgNPs-PLE) causes cell cycle arrest and apoptosis in human prostate (DU145) cancer cells. *Biological Trace Element Research* 2021; 199: 1316–1331 doi: 10.1007/s12011-020-02255-z
4. Coates A, Abraham S, Kaye SB, Sowerbutts T, Frewin C et al. On the receiving end–patient perception of the side-effects of cancer chemotherapy. *European Journal of Cancer and Clinical Oncology* 1983; 19: 203–208. doi: 10.1016/0277-5379(83)90418-2

5. Szakacs G, Paterson JK, Ludwig JA, Booth-Genthe C, Gottesman MM. Targeting multidrug resistance in cancer. *Nature Reviews Drug Discovery* 2006; 5: 219–234. doi: 10.1038/nrd1984
6. Karmous I, Pandey A, Haj KB, Chaoui A. Efficiency of the green synthesized nanoparticles as new tools in cancer therapy: insights on plant-based bioengineered nanoparticles, biophysical properties, and anticancer roles. *Biological Trace Element Research* 2020; 196: 330–342. doi: 10.1007/s12011-019-01895-0
7. Cai Y, Luo Q, Sun M, Corke H. Antioxidant activity and phenolic compounds of 112 traditional Chinese medicinal plants associated with anticancer. *Life Sciences* 2004; 74 (17): 2157–2184. doi: 10.1016/j.lfs.2003.09.047
8. Cragg GM, Newman DJ. Plants as a source of anticancer agents. *Journal of Ethnopharmacology* 2005; 100 (1–2): 72-79. doi: 10.1016/j.jep.2005.05.011
9. Khan F, Pandey P, Ahmad V, Upadhyay TK. *Moringa oleifera* methanolic leaves extract induces apoptosis and G0/G1 cell cycle arrest via down regulation of Hedgehog Signaling Pathway in human prostate PC-3 cancer cells. *Journal of Food Biochemistry* 2020a; 44 (8): e13338. doi: 10.1111/jfbc.13338
10. Ashraf MA. Phytochemicals as potential anticancer drugs: time to ponder nature's bounty. *BioMed Research International* 2020; 2020. doi: 10.1155/2020/8602879
11. Omara T, Kiprof AK, Ramkat RC, Cherutoi J, Kagoya S et al. Medicinal plants used in traditional management of cancer in Uganda: a review of ethnobotanical surveys, phytochemistry, and anticancer studies. *Evidence-Based Complementary and Alternative Medicine* 2020; 15: 3529081. doi: 10.1155/2020/3529081
12. Khan T, Ali M, Khan A, Nisar P, Jan SA et al. Anticancer plants: a review of the active phytochemicals, applications in animal models, and regulatory aspects. *Biomolecules* 2020b; 10 (1): 47. doi: 10.3390/biom10010047
13. Chaudhary LB, Rana TS, Anand KK. Current status of the systematics of *Astragalus* L. (Fabaceae) with special reference to the Himalayan Species in India. *Taiwania* 2008; 53: 338-355. doi: 10.6165/tai.2008.53(4).338
14. Aytaz Z, Ekici M. *Astragalus*. In: Güner, A. et al. (Eds), *Türkiye Bitkileri Listesi (Damarlı Bitkiler)*. Turkey: Nezahat Gökyiğit Botanik Bahçesi ve Flora Araştırmaları, Derneği Yayını, 2012; 427-456.
15. Podlech D, Zarre Sh. [with collaboration of Ekici, M., Maassoumi, A.A. & Sytin, A.]. A taxonomic revision of the genus *Astragalus* L. (Leguminosae) in the Old World. Vols. 1-3. *Naturhistorisches Museum, Wien*, 2013; 2439 pp.
16. Vural M, Subaşı Ü, Ayyıldız G, Samancı İ. Ankara Province Private Geveni (*Astragalus bozakmanii*) Species Conservation Action Plan, Ministry of Forestry and Water Affairs General Directorate of Nature Conservation and National Parks, IX. Regional Directorate-Ankara Branch Office, 2017.
17. Kocabaş YZ, İlçim A, Çömlekçiöğlü N. Kahramanmaraş Başkonuş Mountain Geven (*Astragalus* spp.) And Its Importance, III. International Non-Wood Forest Products Symposium, 8-10 May 2014, Kahramanmaraş.
18. Ibrahim LF, Marzouk MM, Hussein SR, Kawashty SA, Mahmoud K et al. Flavonoid constituents and biological screening of *Astragalus bombycinus* Boiss. *Natural Product Research* 2013; 27: 386–393. doi: 10.1080/14786419.2012.701213
19. Li X, Qu L, Dong Y, Han L, Liu E et al. A review of recent research progress on the *Astragalus* genus. *Molecules* 2014; 19: 18850-18880. doi: 10.3390/molecules191118850
20. Rios JL, Waterman PG. A Review of the pharmacology and toxicology of *Astragalus*. *Phytotherapy Research* 1998; 11: 411-418. doi: 10.1002/(SICI)1099-1573(199709)11:6<411::AID-PTR132>3.0.CO;2-6
21. Calis I, Yuruker A, Tasdemir D, Wright AD, Sticher O et al. Cycloartane triterpene glycosides from the roots of *Astragalus melanophrurius*. *Planta Medica* 1997; 63: 183–186. doi: 10.1055/s-2006-957642
22. Bedir E, Pugh N, Çalış I, Pasco DS, Khan IA. Immunostimulatory effects of cycloartane-type triterpene glycosides from *Astragalus* species. *Biological and Pharmaceutical Bulletin* 2000; 23: 834-837. doi: 10.1248/bpb.23.834
23. Zheng Y, Dai Y, Liu W, Wang N, Cai Y et al. Astragaloside IV enhances taxol chemosensitivity of breast cancer via caveolin-1-targeting oxidant damage. *Journal of Cellular Physiology* 2019; 234: 4277-4290. doi: 10.1002/jcp.27196
24. Zhou X, Liu Z, Long T, Zhou L, Bao Y. Immunomodulatory effects of herbal formula of *Astragalus polysaccharide* (APS) and Polysaccharopeptide (PSP) in mice with lung cancer. *International Journal of Biological Macromolecules* 2018a; 106: 596-601. doi: 10.1016/j.ijbiomac.2017.08.054
25. Zhou R, Chen H, Chen J, Chen X, Wen Y et al. Extract from *Astragalus membranaceus* inhibit breast cancer cells proliferation via PI3K/AKT/mTOR signaling pathway. *BMC Complementary and Alternative Medicine* 2018b; 18: 83-91. doi: 10.1186/s12906-018-2148-2
26. Li W, Hu X, Wang S, Jiao Z, Sun T et al. Characterization and antitumor bioactivity of *Astragalus polysaccharides* by immunomodulation. *International Journal of Biological Macromolecules* 2020; 15: 985-997 doi: 10.1016/j.ijbiomac.2019.09.189

27. Isilar O, Bulut A, Sahin Yaglioglu A, Demirtas I, Arat E et al. Synthesis and biological evaluation of novel urea, thiourea and squaramide diastereomers possessing sugar backbone. *Carbohydrate Research* 2020; 492: 107991 doi: 10.1016/j.carres.2020.107991
28. Kursun Aktar BS, Sicak Y, Tok TT, Emre EE, Sahin Yaglioglu A et al. Designing heterocyclic chalcones, benzoyl/sulfonyl hydrazones: An insight into their biological activities and molecular docking study. *Journal of Molecular Structure* 2020; 1211: 128059. doi: 10.1016/j.molstruc.2020.128059
29. Karakus G, Kaplan Can H, Sahin Yaglioglu A. Synthesis, structural characterization, thermal behavior and cytotoxic/antiproliferative activity assessments of poly(maleic anhydride-alt-acrylic acid)/hydroxyurea polymer/drug conjugate. *Journal of Molecular Structure* 2020; 1210: 127989. doi: 10.1016/j.molstruc.2020.127989
30. Ceylan M, Erkan S, Sahin Yaglioglu A, Akdogan Uremis N, Koç E. Antiproliferative evaluation of some 2-[2-(2-Phenylethenyl)-cyclopent-3-en-1-yl]-1,3-benzothiazoles: DFT and molecular docking study. *Chemistry & Biodiversity* 2020; 17 (4): e1900675. doi: 10.1002/cbdv.201900675
31. Chandra JH, Fritz Z, Eberhard B. Carbon-13 chemical shift assignments of chromones and isoflavones. *Canadian Journal of Chemistry* 1980; 58: 1211-1219. doi: 10.1139/v80-189
32. Kobayashi A, Yata S, Kawazu K. A β -Hydroxychalcone and flavonoids from alfalfa callus stimulated by fungal naphthoquinone, PO-1. *Agricultural and Biological Chemistry* 1988; 52: 223-3227. doi: 10.1080/00021369.1988.10869219
33. Miyazawa M, Ando H, Okuno Y, Araki H. Biotransformation of isoflavones by *Aspergillus niger*, as biocatalyst. *Journal of Molecular Catalysis B: Enzymatic* 2004; 27: 91-95. doi: 10.1016/j.molcatb.2003.09.008
34. Farag MA, Huhman DV, Dixon RA, Sumner LW. Metabolomics reveals novel pathways and differential mechanistic and elicitor-specific responses in phenylpropanoid and isoflavonoid biosynthesis in *Medicago truncatula*. *Cell Cultures^{13C|13W|13O}*. *Plant Physiology* 2008; 146: 387-402. doi: 10.1104/pp.107.108431
35. Chiriac ER, Chitescu CL, Borda D, Lupoe M, Gird CE et al. Comparison of the polyphenolic profile of *Medicago sativa* L. and *Trifolium pratense* L. sprouts in different germination stages using the UHPLC-Q exactive hybrid quadrupole orbitrap high-resolution mass spectrometry. *Molecules* 2020; 25 (10): 149-151. doi: 10.3390/molecules25102321
36. Patron-Gonzalez D, Rios-Gomez R, Flores-Morales V, Rios MY. Metabolites of *Machaerium isadelphum* as chemophenetic markers of *Machaerium* genus. *Biochemical Systematics and Ecology* 2021; 94: 104202. doi: 10.1016/j.bse.2020.104202
37. Lenssen AW, Martin SS, Townsend CE, Hawkins B. Acicerone: An Isoflavone From *Astragalus cicer*. *Phytochemistry* 1994; 36 (5): 1185-1187. https://works.bepress.com/andrew_lenssen/67/
38. Bedir E, Calis I, Aquino R, Piacente S, Pizza C. Trojanoside H: a cycloartane-type glycoside from the aerial parts of *Astragalus trojanus*. *Phytochemistry* 1999; 51: 1017-1020. doi: 10.1016/S0031-9422(99)00035-7
39. Abd El-Latif RR, Shabana MH, El-Gandour AH, Mansour RM, Sharaf MA. New Isoflavone from *Astragalus peregrinus*. *Chemistry of Natural Compounds* 2003; 39: 536-537. doi: 10.1023/B:CONC.0000018105.23722.7d
40. Gülcemal D, Aslanipour B, Bedir E. Secondary Metabolites from Turkish *Astragalus* Species. In: Ozturk M., Hakeem K. (eds) *Plant and Human Health*, Volume 2. Springer, Cham. 2019. doi: 10.1007/978-3-030-03344-6_2
41. Kar S, Akhira A, Chopra S, Ohki S, Karanam B et al. Benzopyrylium salts as new anticancer, antibacterial, and antioxidant agents. *Medicinal Chemistry Research* 2021; 30: 877-885. doi: 10.1007/s00044-020-02685-3
42. Sahin A, Cakmak O, Demirtas I, Okten S, Tutar A. Efficient and selective synthesis of quinoline derivatives". *Tetrahedron* 2008; 64 (43): 10068-10074.
43. Akrawi OA, Mohammed HH, Langer P. 2013. Synthesis and Suzuki—Miyaura Reactions of 3,6,8-Tribromoquinoline: A Structural Revision. *ChemInform Abstract*: doi: 10.1002/chin.201339162
44. Casal JJ, Asis SE. Natural and synthetic quinoline derivatives as antituberculosis. *Agents* 2017; 2 (1): 1007-1009.
45. Starratt AN, Caveney S. Quinoline-2-carboxylic acids from *Ephedra* species. *Phytochemistry* 1996; 4 (5): 1477-1478.
46. Akhmedzhanova VI, Rasulova, KA, Bessonova IA, Shashkov AS, Abdullaev ND et al. A new type quinoline alkaloid from plants of the *Haplophyllum* genus. *Chemistry of Natural Compounds* 2005; 41 (1): 60-64.
47. Li YK, Zhao QJ, Hu J, Zou Z, He XY et al. Two New quinoline alkaloid mannopyranosides from *Solidago canadensis*. *Helvetica* 2009; 92 (5): 928-931.
48. Kumar R, Duffy S, Avery VA, Carroll AR, Davis RA. Microthecaline a, a quinoline serrulatane alkaloid from the roots of the australian desert plant *Eremophila microtheca*. *Journal of Natural Products* 2018; 81 (4): 1079-1083.
49. Yamashita M, Saito Y, Rahim A, Fukuyoshi S, Miyake K et al. Novel furoquinolinones from an Indonesian Plant, *Lunasia amara*. *Tetrahedron Letters* 2020; 61 (20): 151861.

50. Robertson LP, Makwana V, Voser TM, Holland DC, Carroll AR. Leptanoine D, a new quinoline alkaloid from the Australian tree *Pitaviaster haplophyllus* (Rutaceae). *Australian Journal of Chemistry* 2021; 74 (3), 173-178.
51. Wulff P, Carle JS, Christophersen C. Marine alkaloids—6. The first naturally occurring bromo-substituted quinoline from *Flustra foliacea*. *Comparative Biochemistry and Physiology Part B: Comparative Biochemistry* 1982; 71 (3): 525-526.
52. Website <https://chemistry.stackexchange.com/questions/103925/exceptions-to-the-nitrogen-rule-in-mass-spectrometry> [accessed 16.09.2021].
53. Separation Science (2021). [online]. Website <https://blog.sepscience.com/massspectrometry/the-role-of-isotope-peak-intensities-obtained-using-mass-spectrometry-in-determining-an-elemental-composition-part-2> [accessed 06.04.2021].
54. Moreno J, Fatela F, Leorri E, Araujo MF, Moreno F et al. Bromine enrichment in marsh sediments as a marker of environmental changes driven by Grand Solar Minima and anthropogenic activity (Caminha, NW of Portugal). *Science of the Total Environment* 2015; 506–507; 554–566. doi: 10.1016/j.scitotenv.2014.11.062
55. McCall AS, Cummings CF, Bhavé G, Vanacore R, Page-McCaw A et al. Bromine is an essential trace element for assembly of collagen IV scaffolds in tissue development and architecture. *Cell* 2014; 157: 1380–1392. doi: 10.1016/j.cell.2014.05.009
56. Shtangeeva I, Niemela M, Peramaki P. Effects of bromides of potassium and ammonium on some crops. *Journal of Plant Nutrition* 2019; 42: 2209–2220. doi: 10.1080/01904167.2019.1655037
57. Gribble GW. The diversity of naturally occurring organobromine compounds. *Chemical Society Reviews* 1999; 28: 335–346. doi: 10.1039/A900201D
58. Karagöz A, Turgut-Kara N, Çakır Ö, Demirgan R, Arı Ş. Cytotoxic Activity of Crude Extracts from *Astragalus chrysochlorus* (Leguminosae). *Biotechnology & Biotechnological Equipment* 2007; 21(2): 220-222.
59. Jozwiak M, Filipowska A, Fiorino F, Struga M. Anticancer activities of fatty acids and their heterocyclic derivatives. *European Journal of Pharmacology* 2020; 871: 172937.
60. Al-Snafi AE. Chemical constituents and pharmacological effects of *Astragalus hamosus* and *Astragalus tribuloides* grown in Iraq. *Asian Journal of Pharmaceutical Sciences* 2015; 5 (4): 321-328.
61. Krasteva I, Platikanov S, Nikolov S, Kaloga M. Flavonoids from *Astragalus hamosus*. *Natural Product Research* 2007; 21 (5): 392-395 doi: 10.1080/14786410701236871
62. Krasteva I, Momekov G, Zdraveva P, Konstantinov S, Nikolov S. Antiproliferative effects of a flavonoid and saponins from *Astragalus hamosus* against human tumor cell lines. *Pharmacognosy Magazine* 2008; 4: 269-272. <http://www.phcog.com/text.asp?2008/4/16/269/57997>
63. Shaikh AM, Shrivastava B, Apte KG, Navale SD. Medicinal plants as potential source of anticancer agents: a review. *Journal of Pharmacognosy and Phytochemistry*. 2016; 5 (2): 291-295.
64. Liu C, Wang K, Zhuang J, Gao C, Li H et al. The modulatory properties of *Astragalus membranaceus* treatment on triple-negative breast cancer: an integrated pharmacological method. *Frontiers in Pharmacology* 2019; 10: 1171-1184. doi: 10.3389/fphar.2019.01171
65. Mehraban F, Mostafazadeh M, Sadeghi H, Azizi A, Toori MA et al. Anticancer activity of *Astragalus ovinus* against 7, 12 dimethyl benz (a) anthracene (DMBA)-induced breast cancer in rats. *Avicenna Journal of Phytomedicine* 2020; 10 (5): 533–545. PMID: PMC7508319
66. Al-Harbi NA, Awad NS, Alsberi HM, Abdein MA. Apoptosis Induction, Cell Cycle Arrest and in vitro Anticancer Potentiality of *Convolvulus spicatus* and *Astragalus vogelii*. *World*. 2019; 8: 69–75.
67. Zhu J, Zhang H, Zhu Z, Zhang Q, Ma X et al. Effects and mechanism of flavonoids from *Astragalus complanatus* on breast cancer growth. *Naunyn-Schmiedeberg's Archives of Pharmacology* 2015; 388: 965–972. doi: 10.1007/s00210-015-1127-0
68. Gupta M, Jun Lee H, Barden CJ, Weaver DF. The Blood–Brain Barrier (BBB) Score. *Journal of Medicinal Chemistry* 2019; 62 (21): 9824–9836. doi: 10.1021/acs.jmedchem.9b01220
69. Shweta M, Rashmi D. In vitro ADME studies of TUG-891, a GPR-120 inhibitor using Swiss ADME predictor. *Journal of Drug Delivery Science and Technology* 2019; 9 (2-S): 266-369. DOI doi: 10.22270/jddt.v9i2-s.2710

Supplementary materials

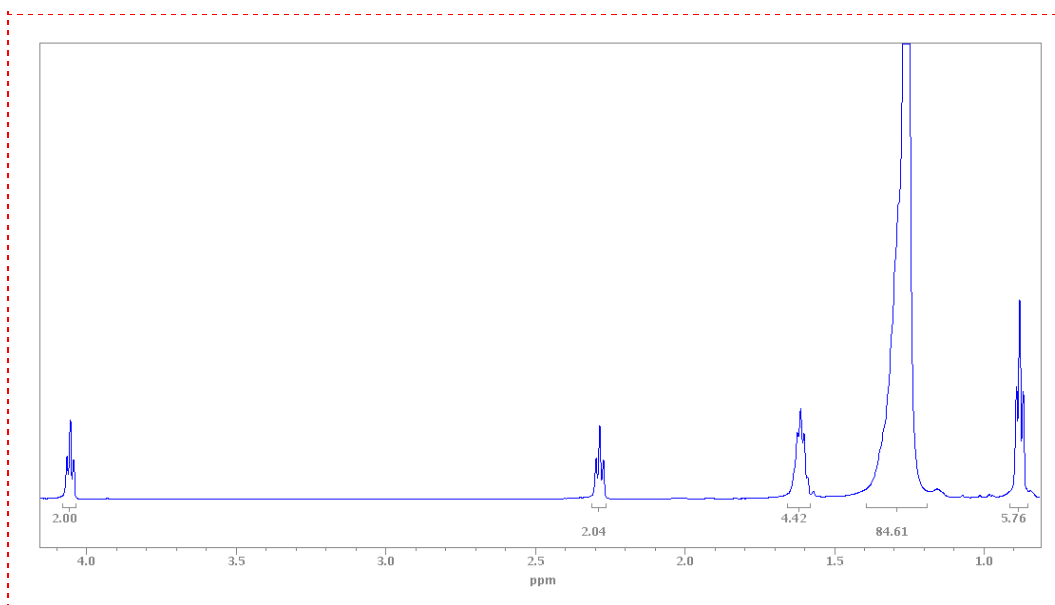
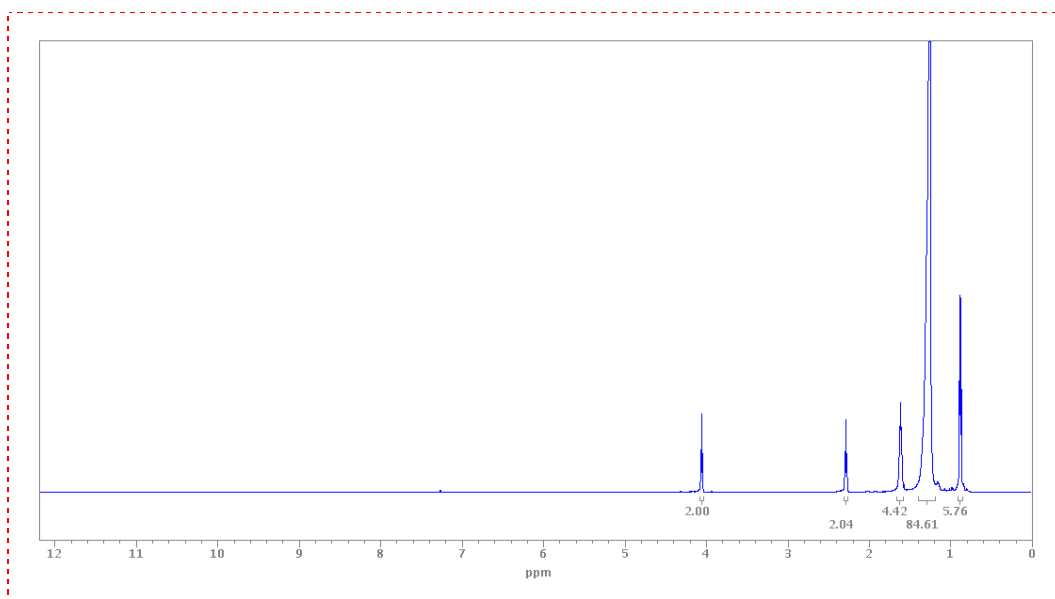
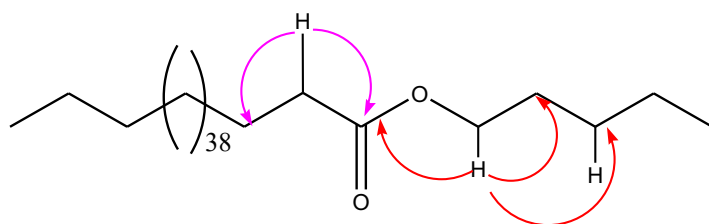


Figure S1. ^1H NMR spectrum and HMBC correlations of compound **1** (600 MHz, CDCl_3)

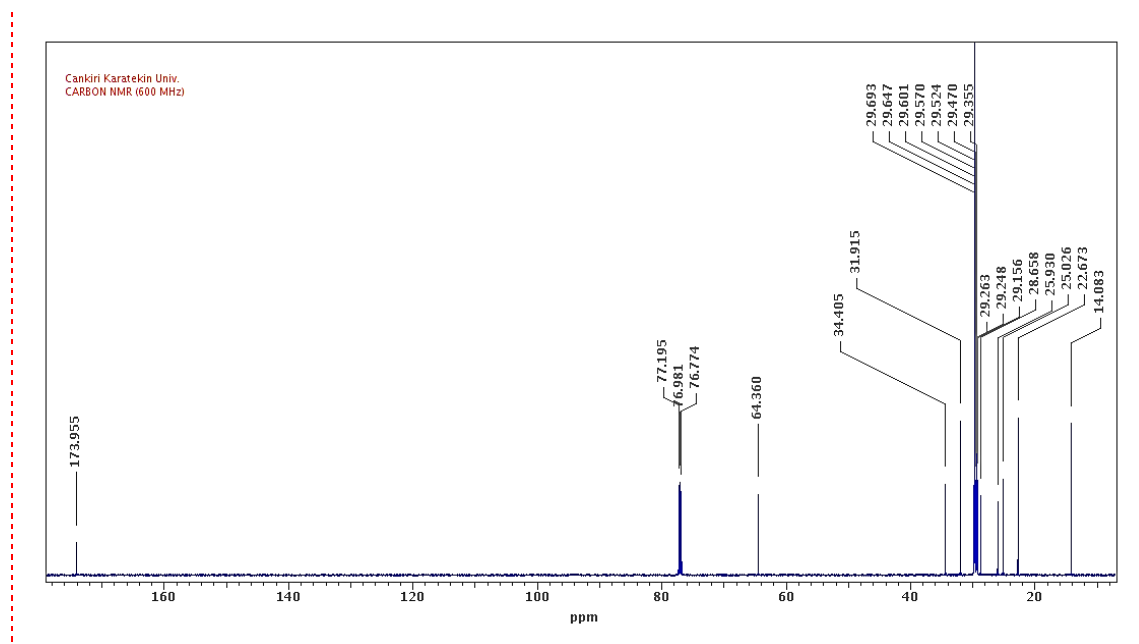


Figure S2. ^{13}C NMR spectrum of compound **1** (150 MHz, CDCl_3)

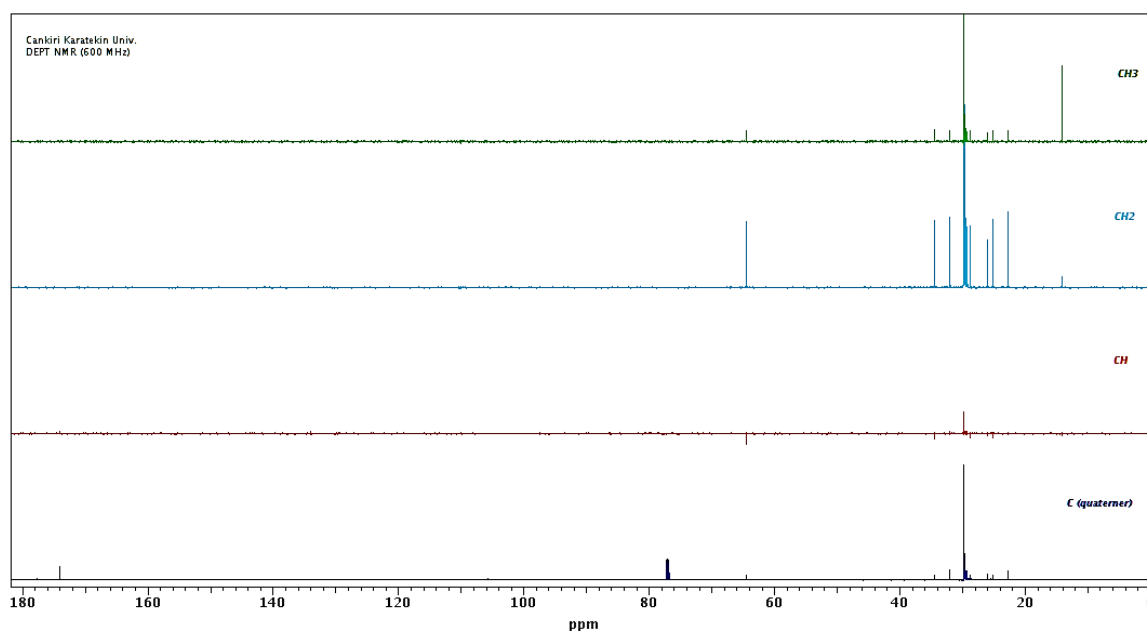


Figure S3. DEPT NMR spectrum of compound **1** (150 MHz, CDCl_3)

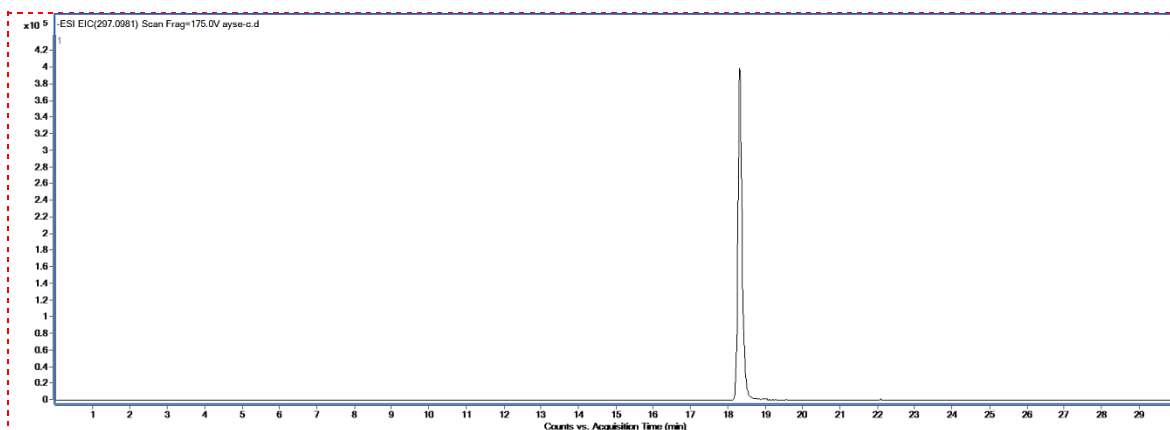


Figure S4. HPLC/TOF-MS chromatogram of compound **2**

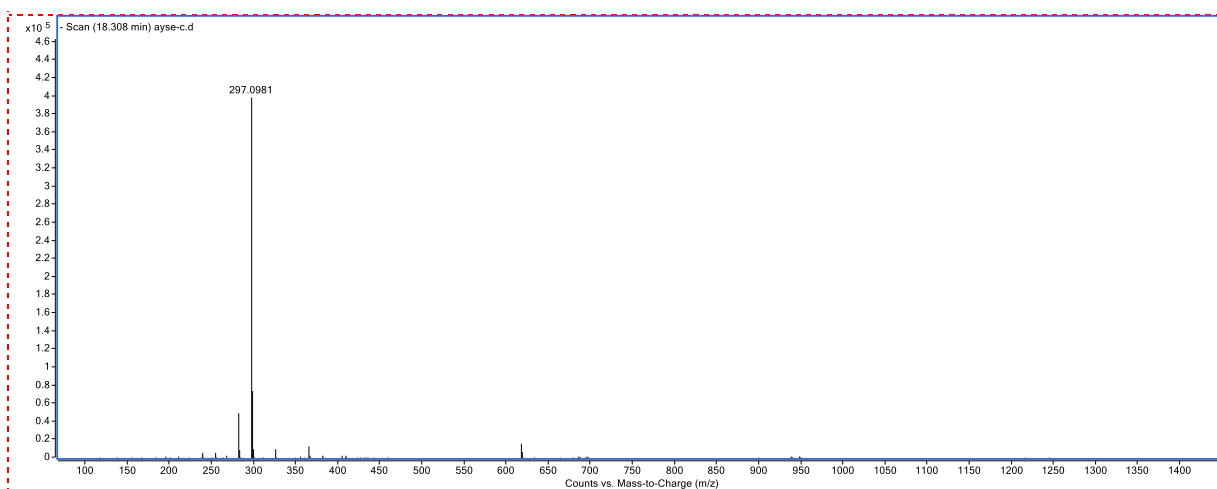


Figure S5. Mass spectrum of compound **2**

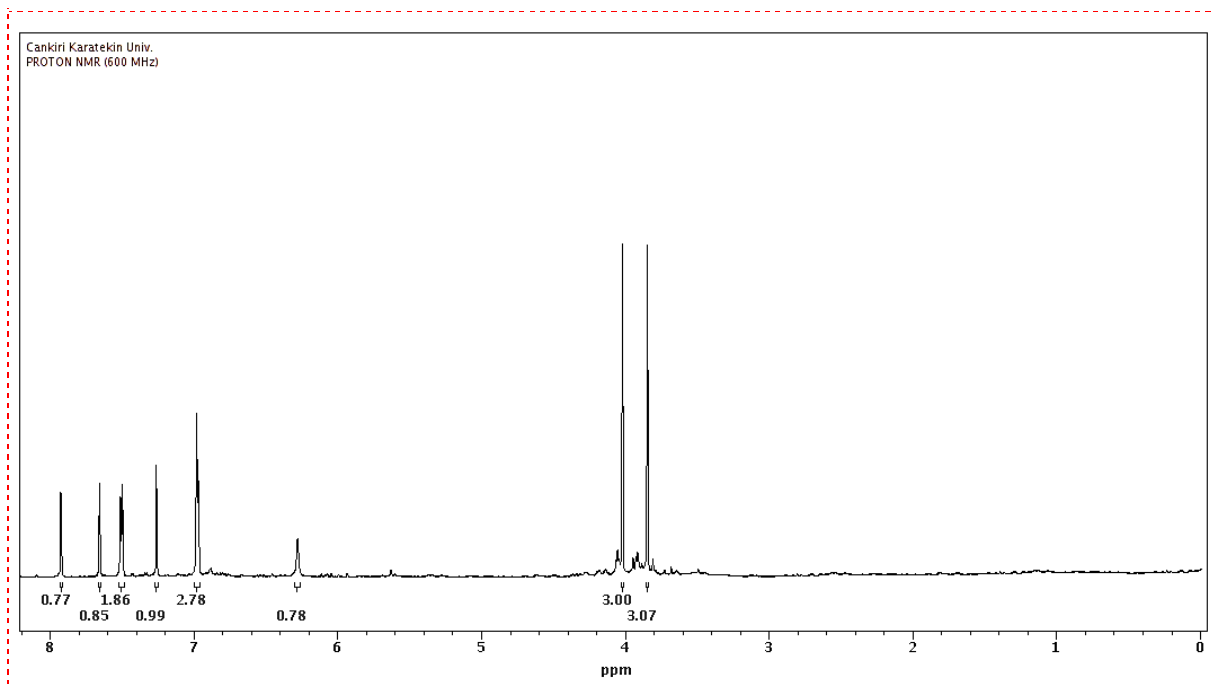
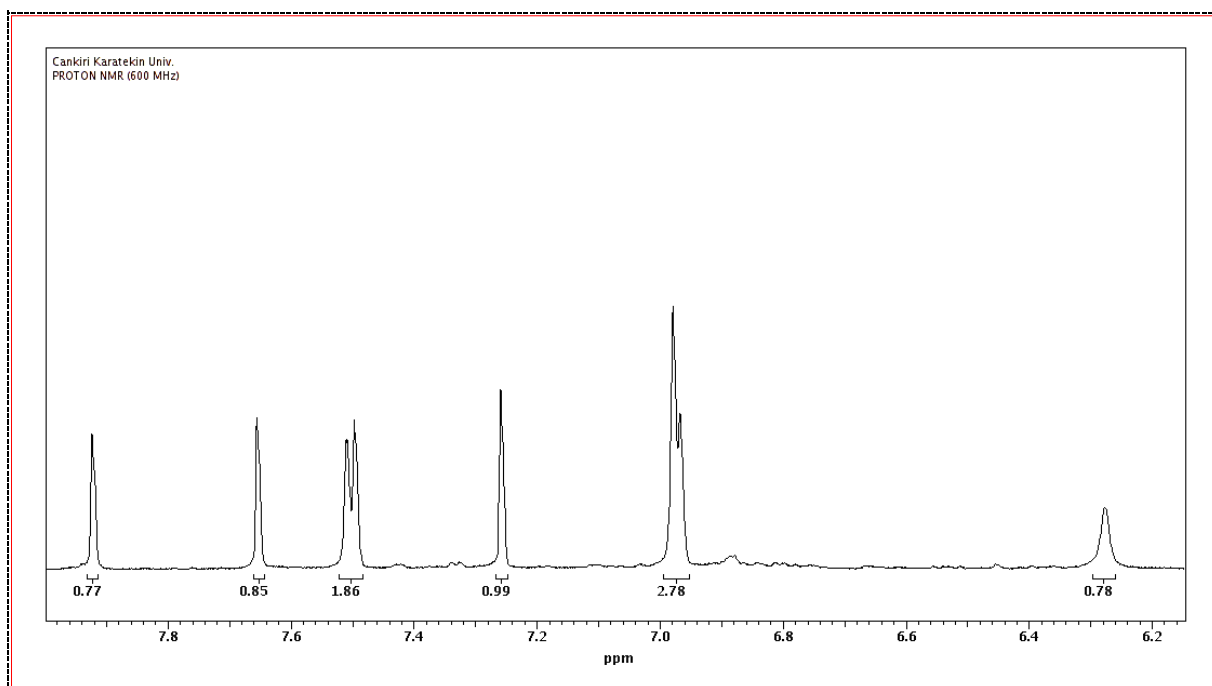


Figure S6. ^1H NMR spectrum of compound **2** (600 MHz, CDCl_3)

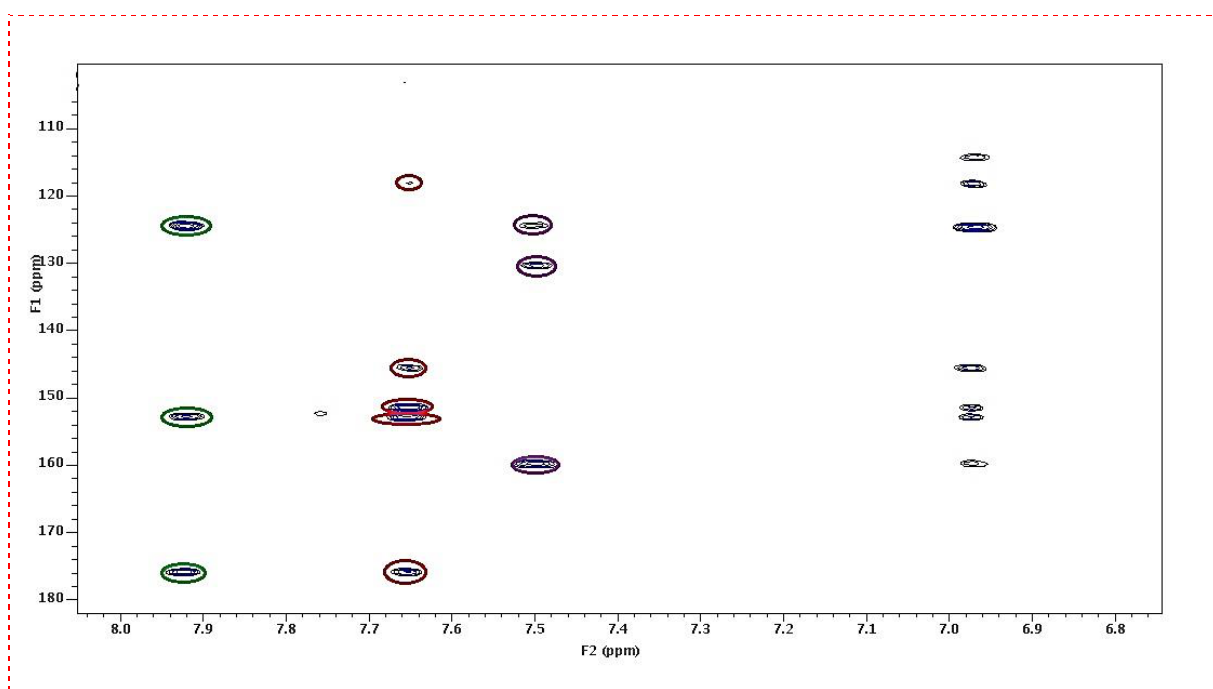
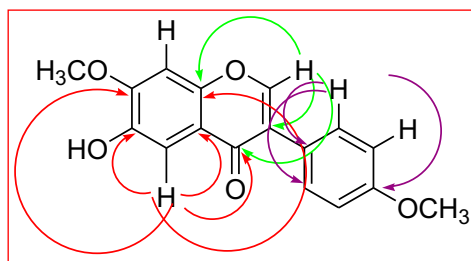


Figure S7. HMBC spectrum of compound **2** (600 MHz, CDCl₃)

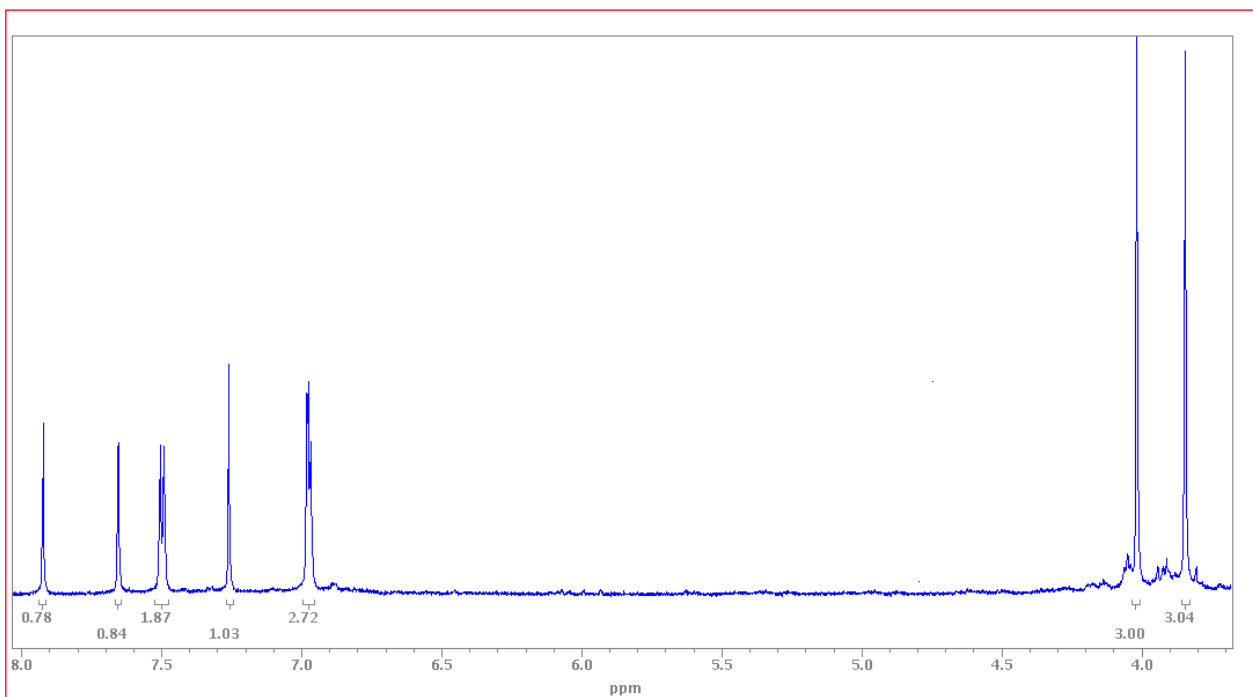


Figure S8. ¹H NMR spectrum of compound **2** taken with D₂O (600 MHz, CDCl₃)

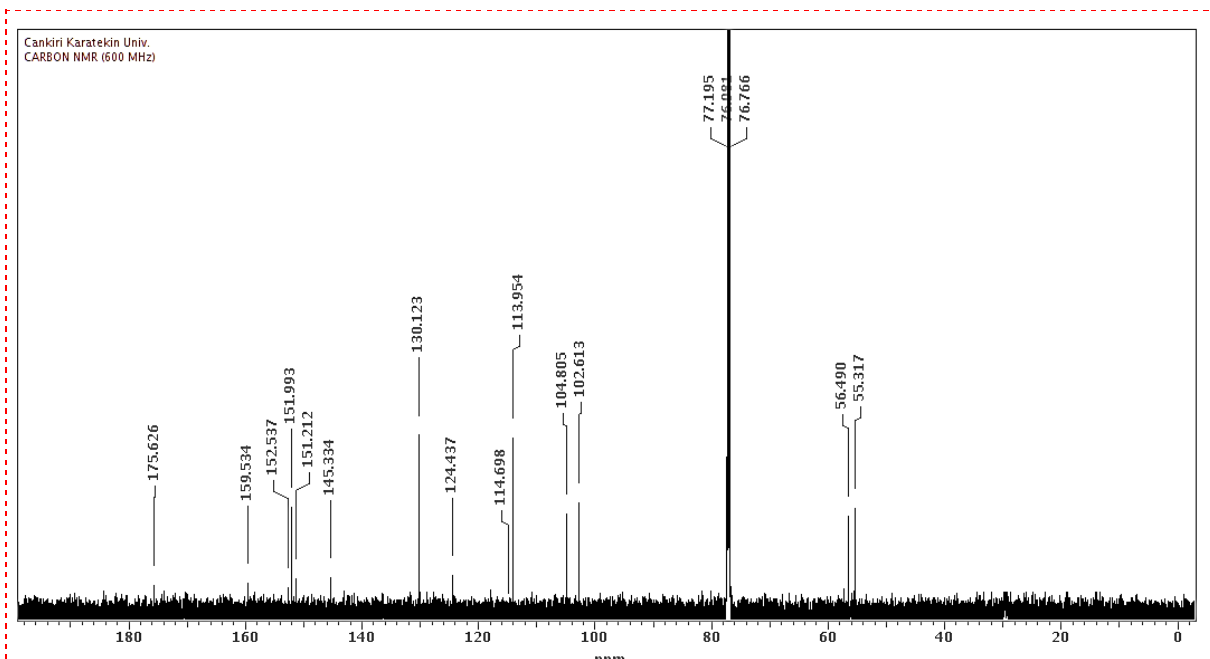


Figure S9. ^{13}C NMR spectrum of compound **2** (150 MHz, CDCl_3)

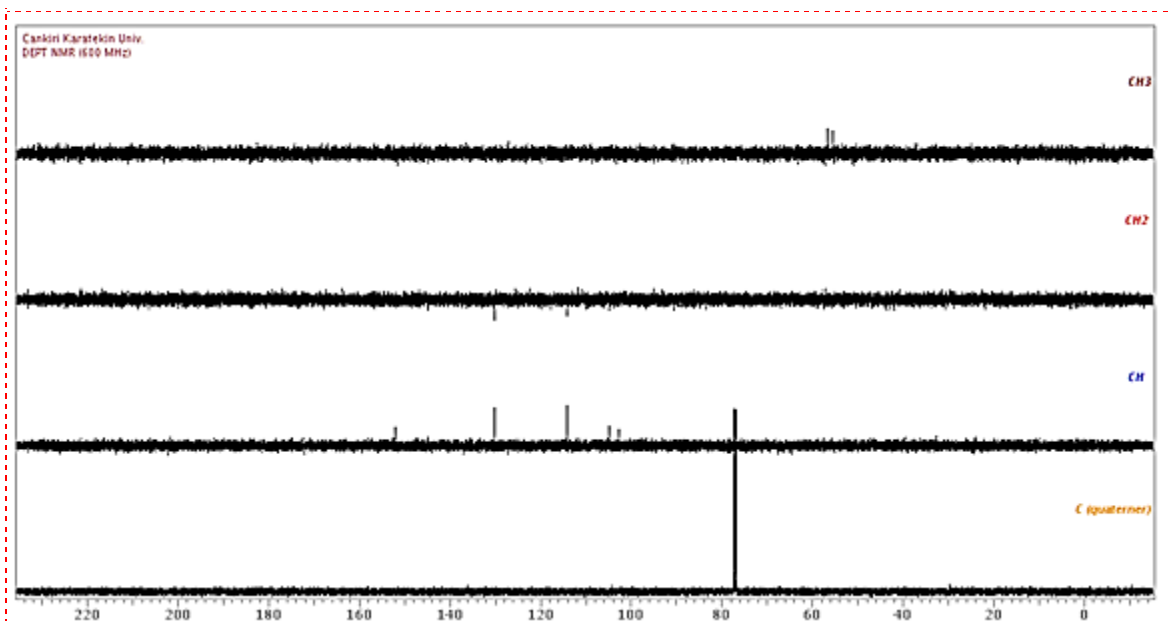


Figure S10. DEPT NMR spectrum of compound **2** (150 MHz, CDCl_3)

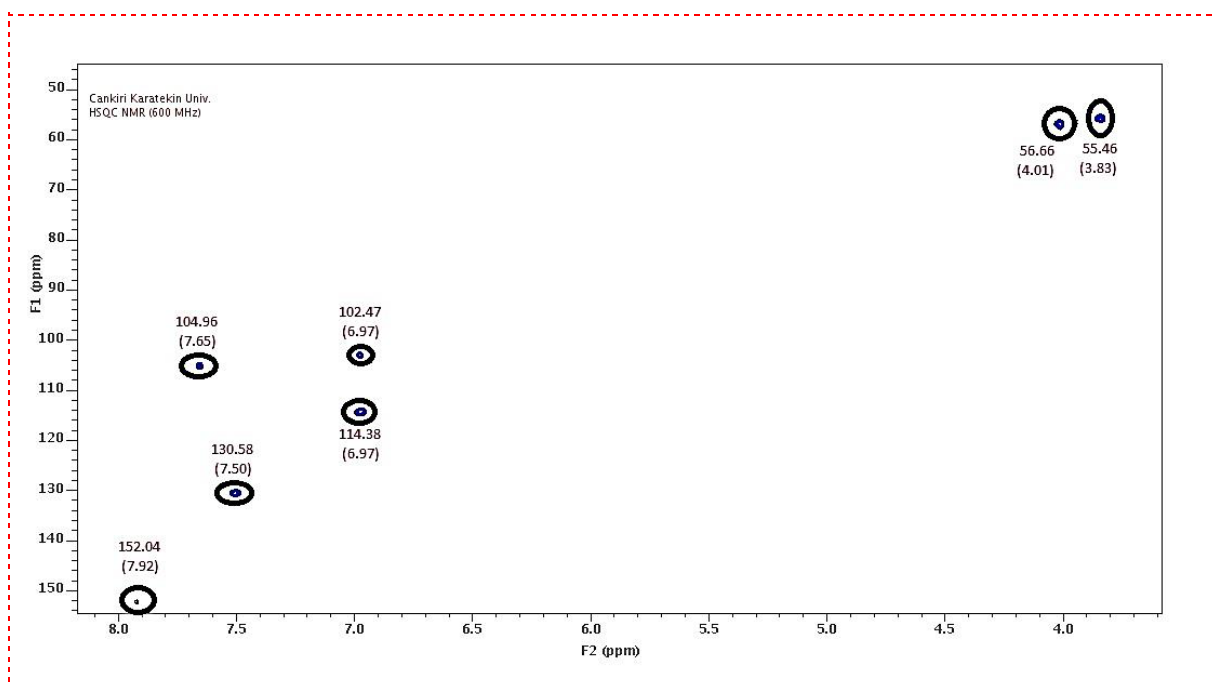


Figure S11. HSQC NMR spectrum of compound **2** (600 MHz, CDCl₃)

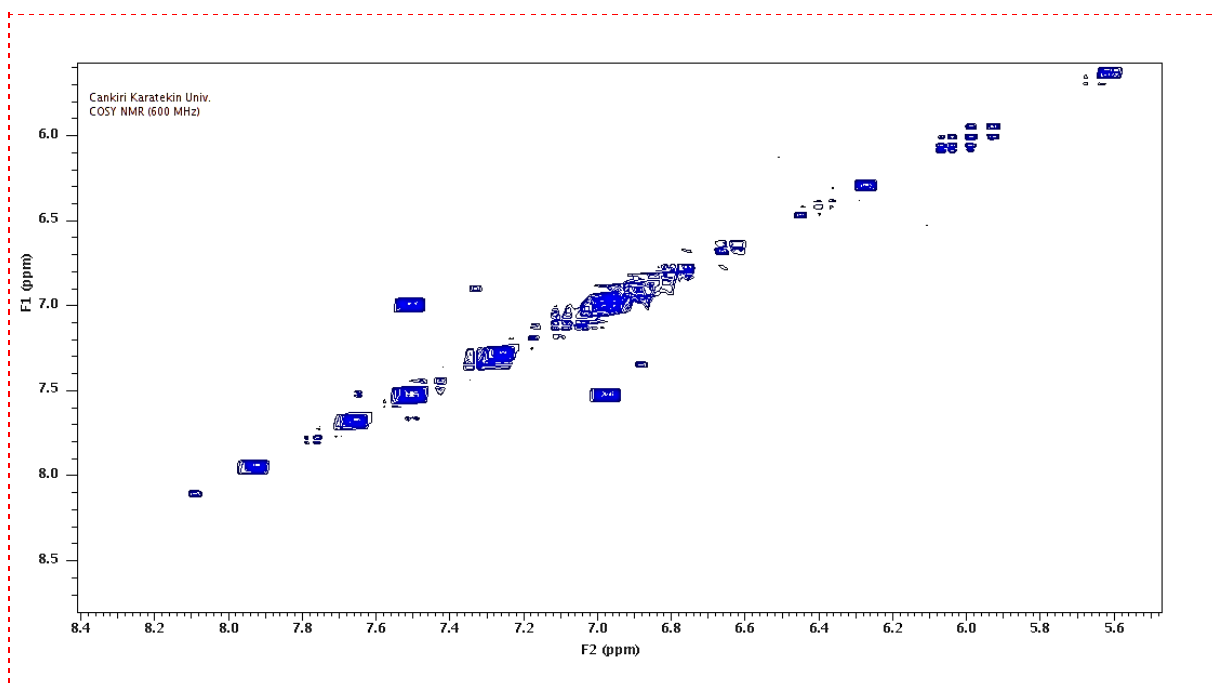


Figure S12. COSY NMR spectrum of compound **2** (600 MHz, CDCl₃)

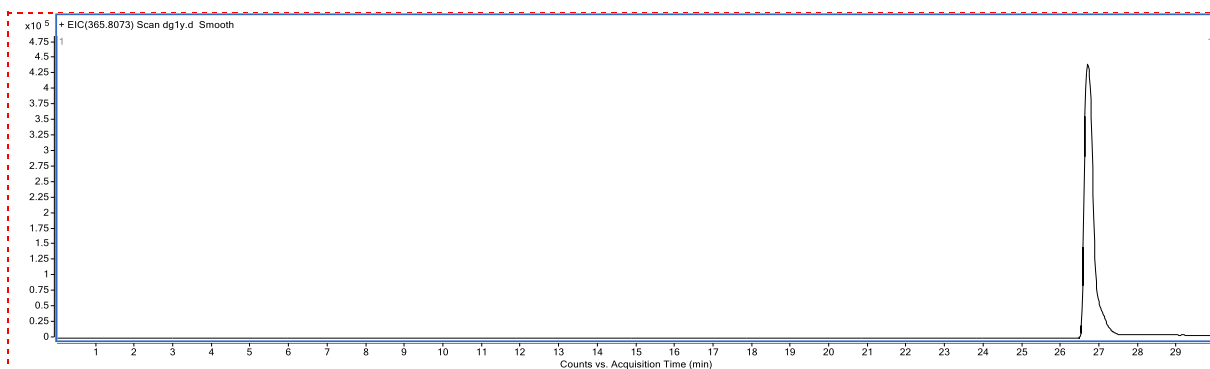


Figure S13. HPLC/TOF-MS chromatogram of compound 3-4 mix

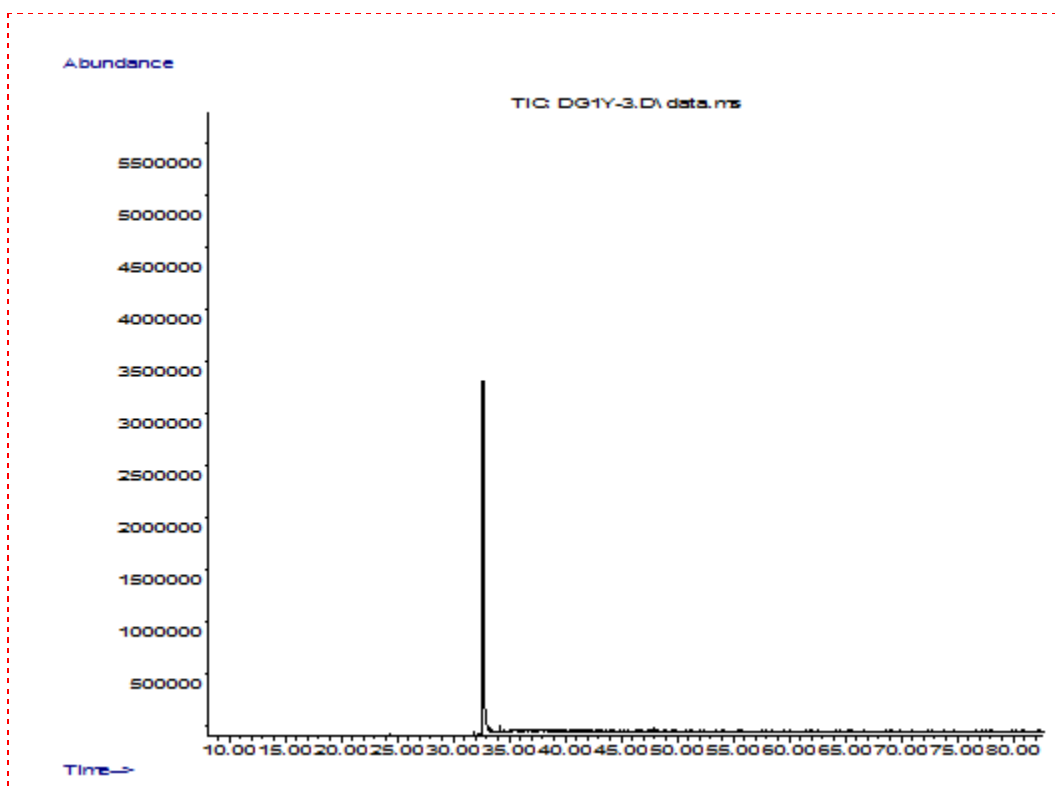


Figure S14. GC-MS chromatogram of compound 3-4 mix

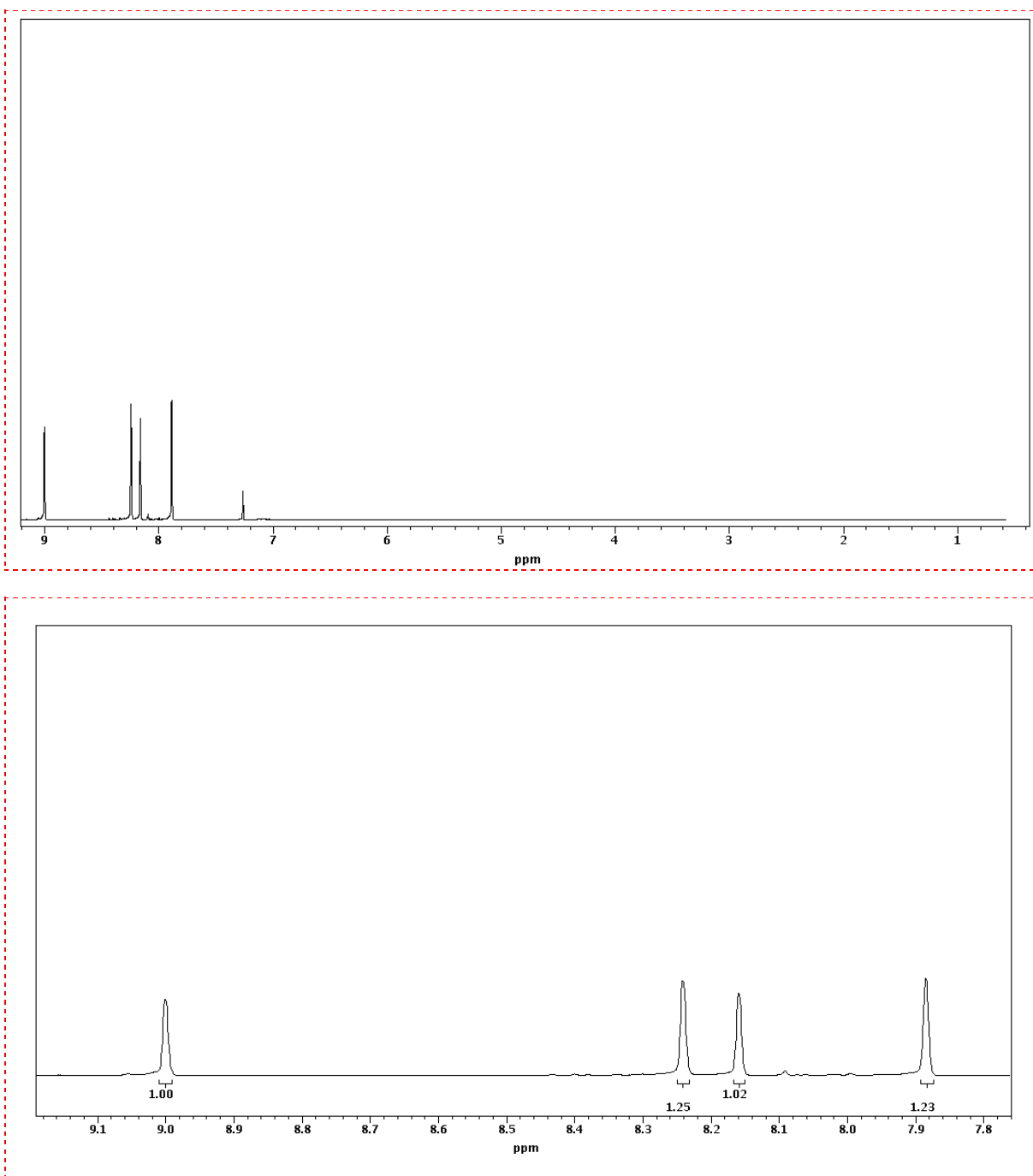


Figure S15. ¹H NMR spectrum of compound 3-4 mix (600 MHz, CDCl₃)

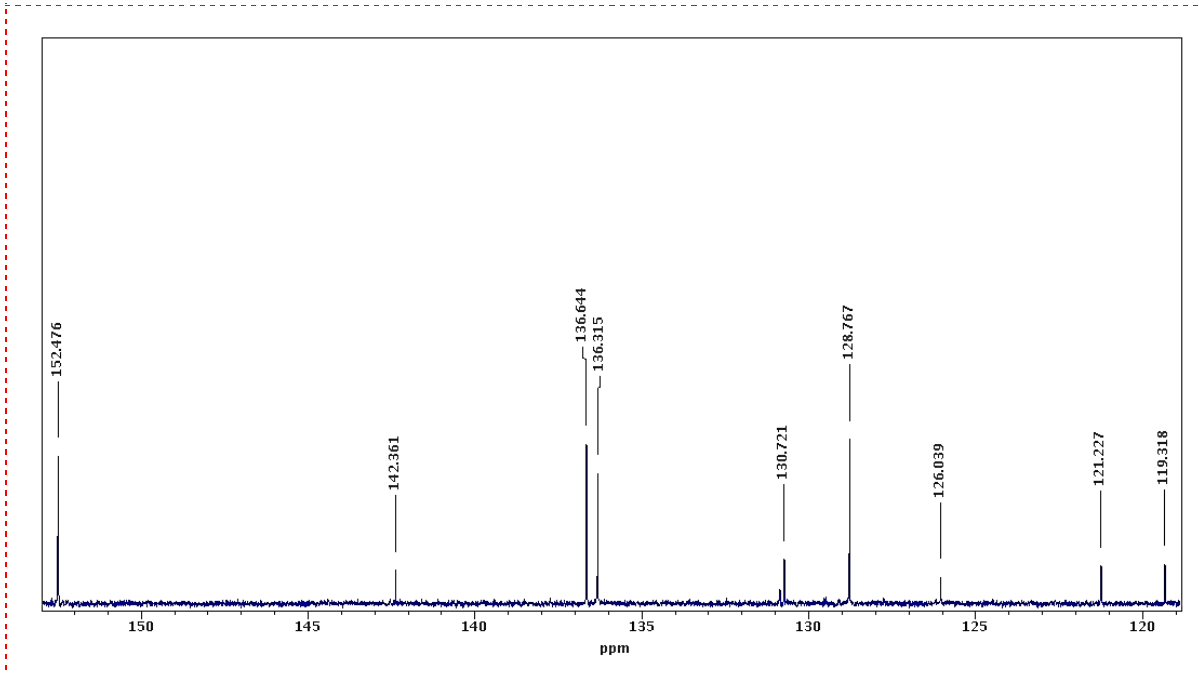
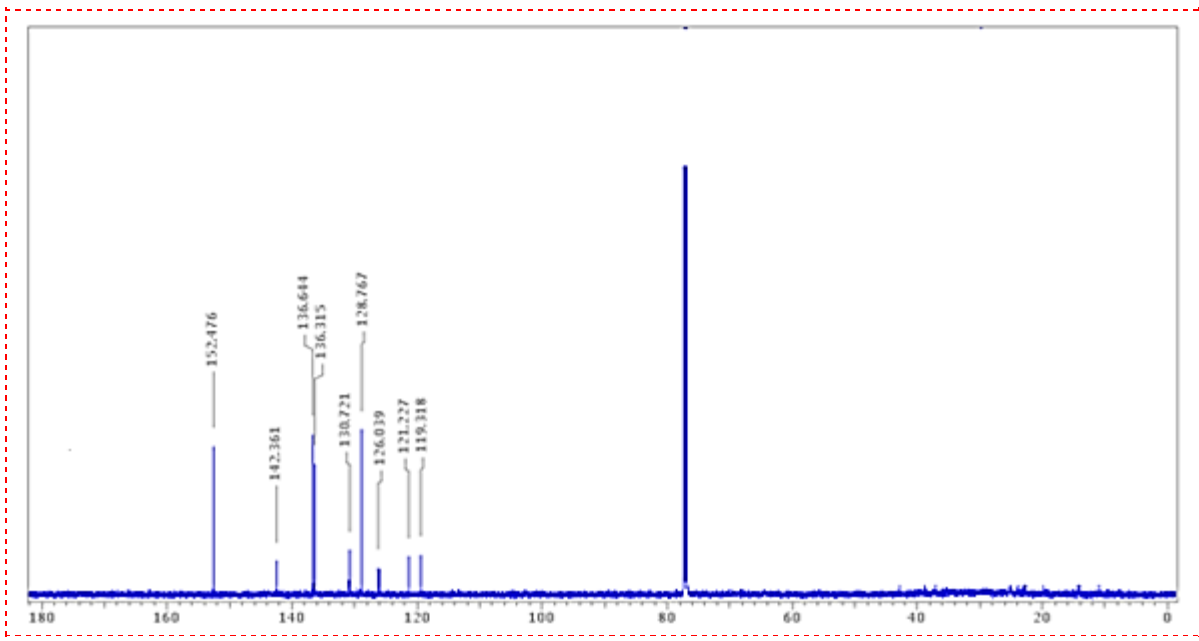


Figure S16. ^{13}C NMR spectrum of compound 3-4 mix (150 MHz, CDCl_3)

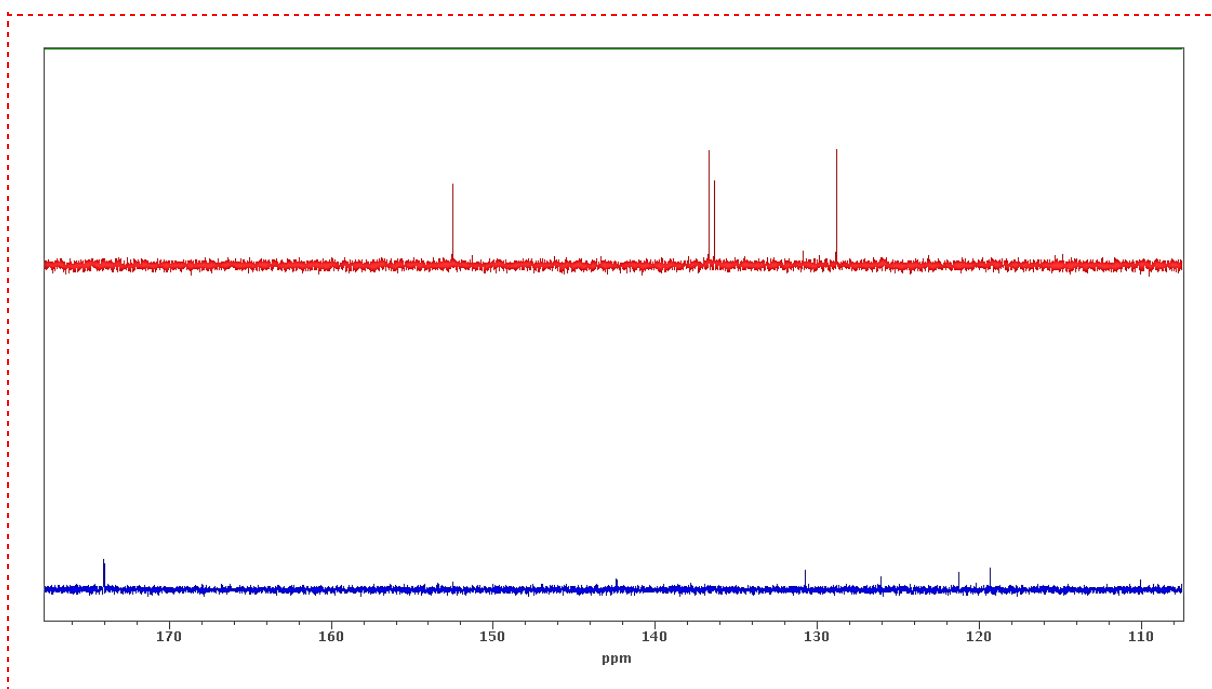


Figure S17. DEPT NMR spectrum of compound **3-4** mix (150 MHz, CDCl_3)

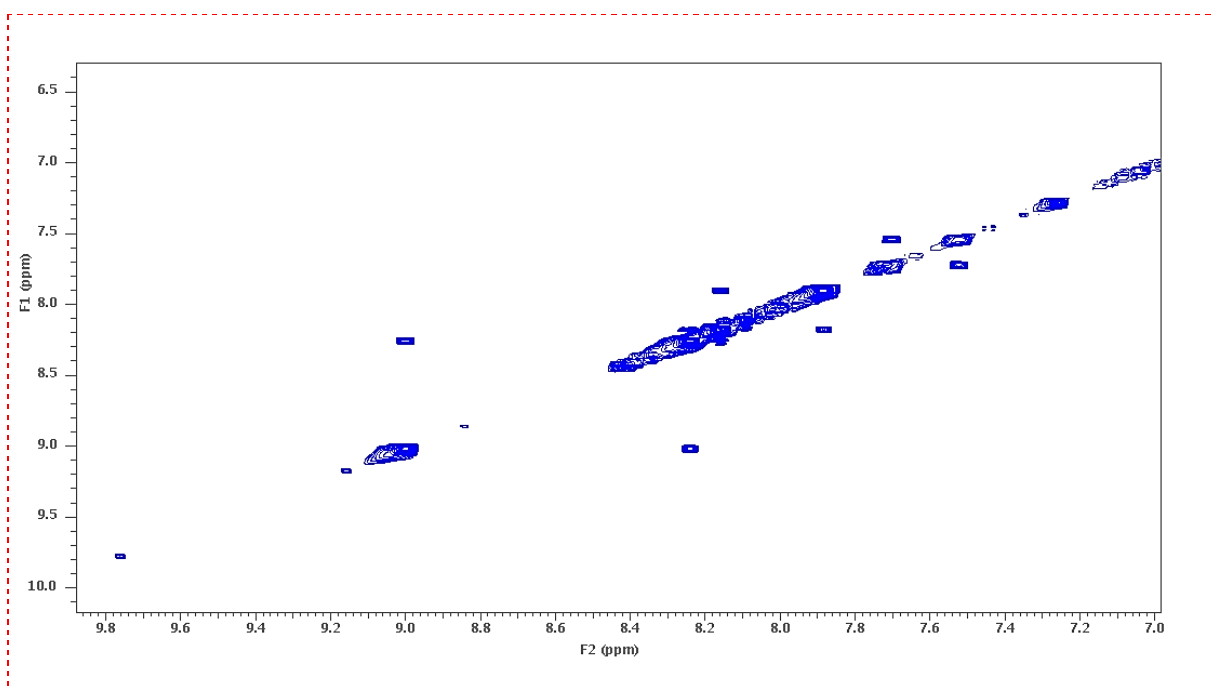


Figure S18. COSY spectrum of compound **3-4** mix (600 MHz, CDCl_3)

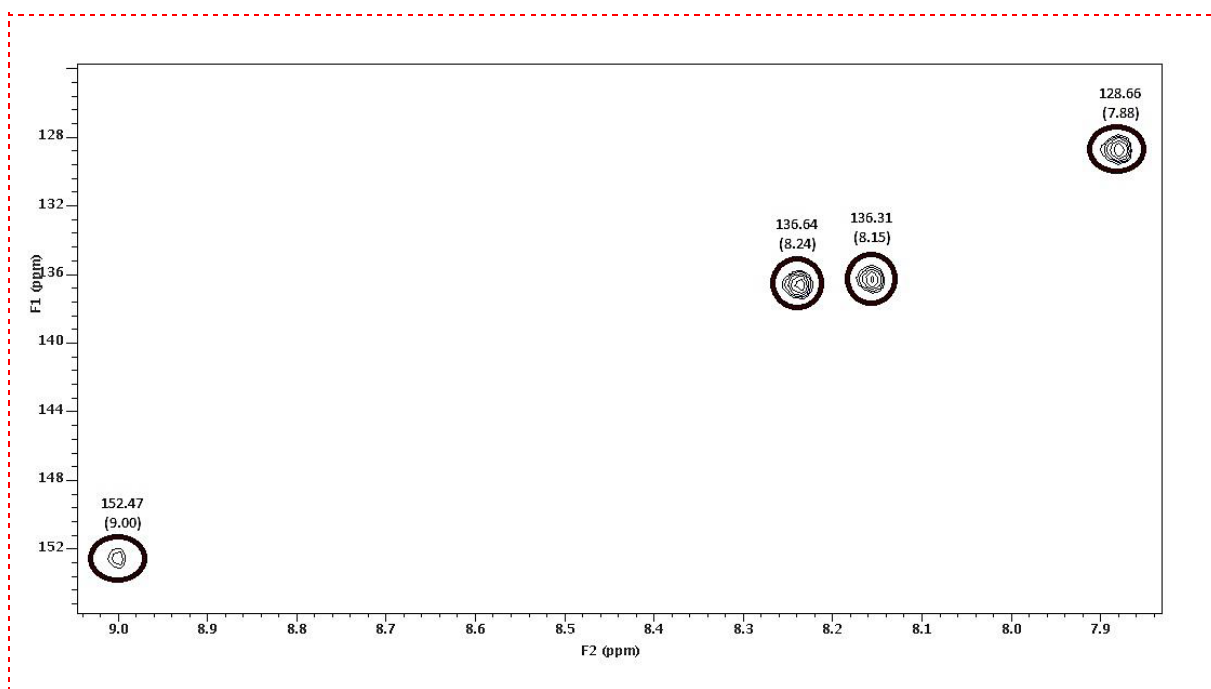
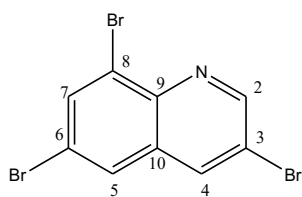
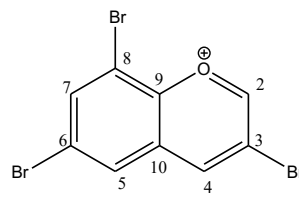


Figure S19. HSQC spectrum of compound 3-4 mix (600 MHz, CDCl₃)



Compound 3



Compound 4

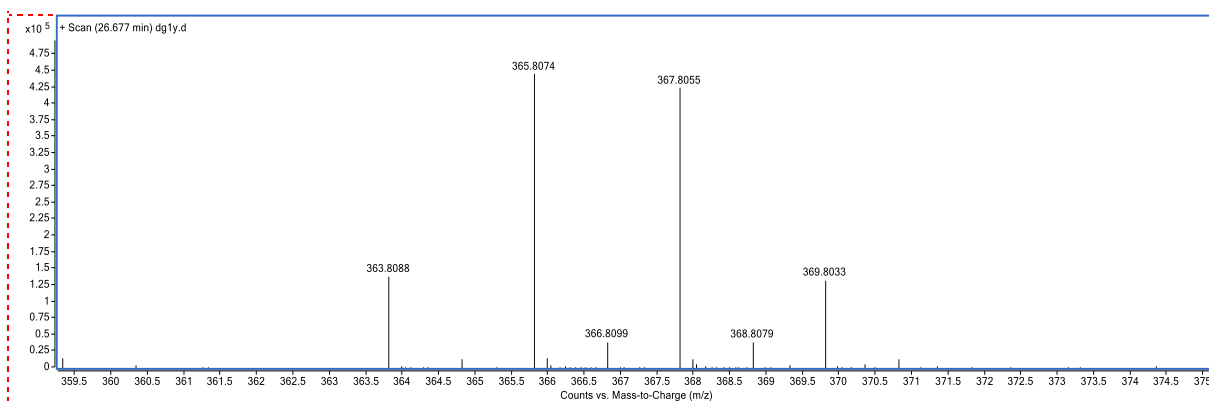
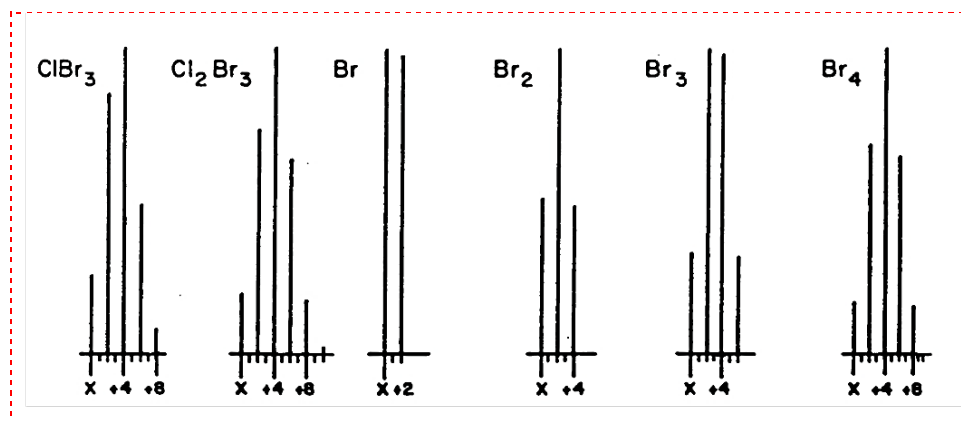


Figure S20. The mass spectra and structure of compound 3-4 mix

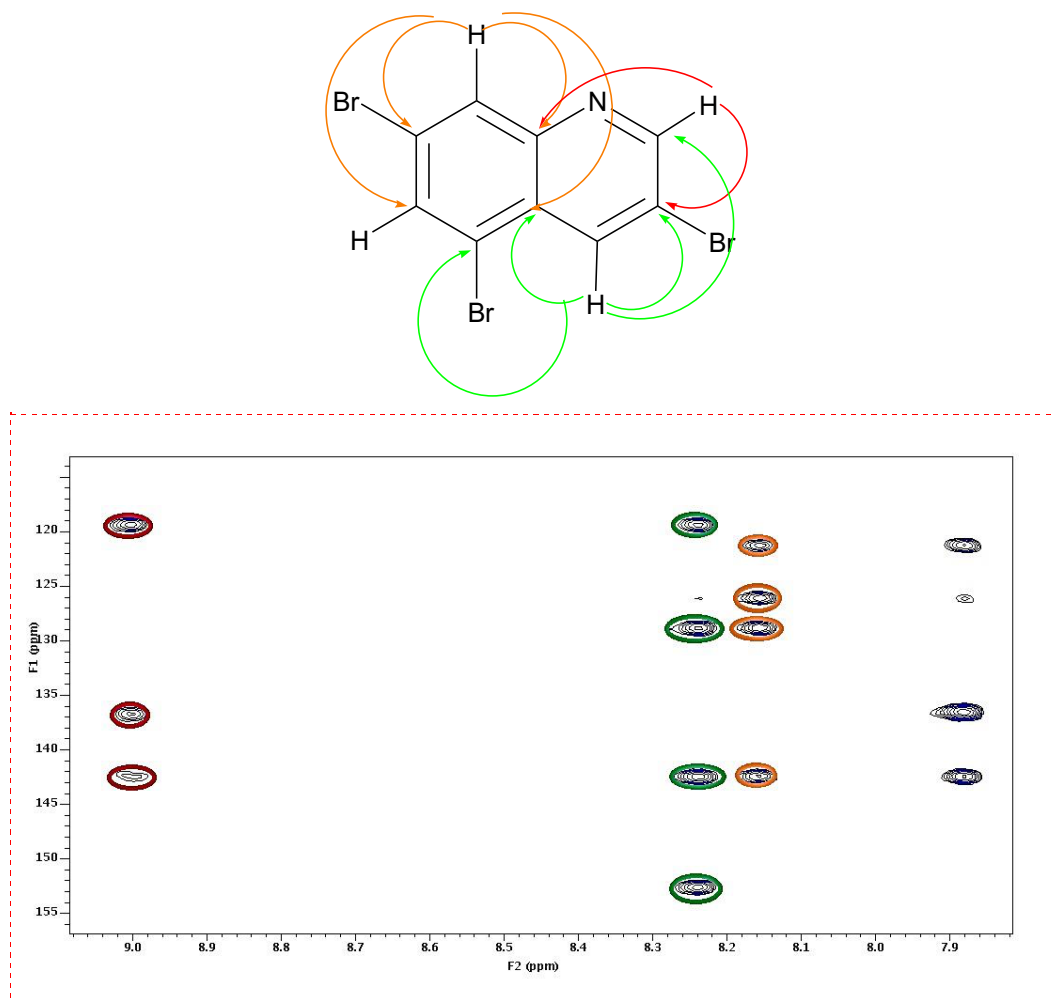
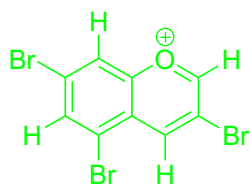
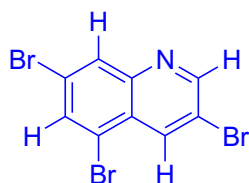
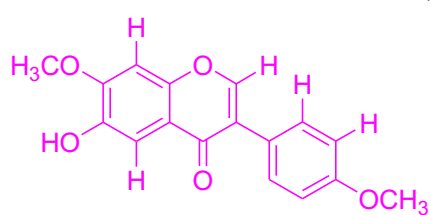
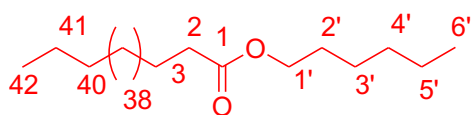


Figure S21. HMBC NMR spectrum and correlations of compound **3-4** mix (600 MHz, CDCl₃)

Table S1. ^1H , ^{13}C NMR, and DEPT data of compound **2**

Position	^1H	^{13}C	DEPT
Compound 2			
2	7.92 (1H, <i>s</i>)	152.04	CH
3	-	124.17	C
4	-	175.65	C
5	7.65 (1H, <i>s</i>)	104.96	CH
6	-	145.53	C
7	-	152.45	C
8	6.97 (1H, <i>s</i>)	102.47	CH
8a	-	151.15	C
4a	-	117.93	C
1'	-	124.31	C
2'	7.50 (2H, <i>dt</i> , $J=2.0$, 8.0 Hz)	130.58	CH
3'	6.97 (2H, <i>dt</i> , $J=2.0$, 8.0 Hz)	114.38	CH
4'	-	159.49	C
5'	6.97 (2H, <i>dt</i> , $J=2.0$, 8.0 Hz)	114.38	CH
6'	7.50 (2H, <i>dt</i> , $J=2.0$, 8.0 Hz)	130.58	CH
OMe	3.83 (3H, <i>s</i>)	55.46	CH ₃
	4.01 (3H, <i>s</i>)	56.66	CH ₃
OH	6.27 (1H, <i>s</i>)	-	-



1

2

3

4

	IC50 against C6 cell	Cytotoxicity %
1	4.50	24
2	2.81	43
3+4	4.33	4
5-FU	5.8	39

Highlights

1. Four compound were isolated firstly from *Astragalus leucothrix*.
2. Two tribromo compound was identified for the first time as a natural product.
3. According to Lipinski's rule of five; 2 -4 could be a new potential anticancer agent.